EEE 588: Design of Multivariable Control Systems **Spring 2019**

AV-8A Harrier Aircraft Longitudinal Dynamics

Advisor: Dr. Armando Rodriguez *Student: Sambarta Ray-1215219161*

1 Overview

Background: The McDonnell Douglas(now Boeing) AV-8A Harrier is a single engine ground attack aircraft which is capable of vertical or short takeoff and landing. It was developed in the 1960s and formed the first generation of the Harrier series of aircrafts. It is powered by a single Pegasus turbofan engine mounted in the fuselage. The engine is fitted with four vectoring nozzles for directing the thrust generated(two for the bypass flow and two for the jet exhaust) and two air intakes. The aircraft also has several smaller reaction nozzles in the nose , tail and wingtips for the purpose of balancing during vertical flight. The aircraft is capable of forward flight like a fixed wing aircraft. It is also capable of doing VTOL and STOL manoeuvres where the lift and control surfaces are useless. The harrier also has two control elements namely the thrust vector and the reaction control system which is not found in conventional fixed-wing aircraft.

2 Modelling

2.1 Linearized plant model

To study the properties of various types of MIMO control design we use the linearized plant model of the Harrier Aircraft for longitudinal dynamics. The plant has been obtained from the AAR's Linear Systems book [1]. The model taken in the book is a simplified small signal model for AV-8A Harrier Aircraft, linearized at a medium speed flight condition. The TITO model for the longitudinal dynamics at the above flight conditions is as follows:

$$\dot{x} = \mathbf{A}x + \mathbf{B}u \tag{1}$$

$$y = \mathbf{C}x + \mathbf{D}u \tag{2}$$

$$A = \begin{bmatrix} 0 & 1.0000 & 0 & 0 & 0 & 0 \\ -1.8370 & -1.8930 & 1.8370 & -0.0004 & 0.0062 & -0.1243 \\ 0.5295 & 0.0085 & -0.5295 & 0.0006 & 0.0002 & 0.0017 \\ -34.5 & 0 & 2.3000 & -0.0621 & 0.4209 & -0.0452 \\ 0 & 0 & 0 & 0 & -1.9660 & 0 \\ 0 & 0 & 0 & 0 & 0 & -12.0000 \end{bmatrix}, \tag{3}$$

$$B = \begin{bmatrix} 0 & 0 \\ 0 & 0 \\ 0 & 0 \\ 0 & 0 \\ 1.966 & 0 \\ 0 & 12 \end{bmatrix}, C = \begin{bmatrix} 0 & 0 & 0 & 1.0000 & 0 & 0 \\ 0 & 0 & 57.2958 & 0 & 0 & 0 \end{bmatrix} \tag{4}$$

$$u = \begin{bmatrix} \delta_s\text{—stick input} \\ \delta_t\text{—throttle} \end{bmatrix}, x_p = \begin{bmatrix} \theta\text{—pitch angle} \\ q\text{—pitch rate} \\ \gamma\text{—flight path angle} \\ v\text{—velocity} \\ s_a\text{—stabilizer angle} \\ N\text{—enginefan speed} \end{bmatrix}, y_p = \begin{bmatrix} v\text{—velocity} \\ \gamma\text{—flight path angle} \end{bmatrix} \tag{5}$$

2.2 Actuator Dynamics

- **Control Flutter** When an aerodynamic control surface is deflected, the cambered side experiences a low pressure zone in accordance with Bernoulli's principle and the control surface will naturally attempt to reallign itself with mounting surface when its free to move. Sometimes the center of gravity with a control surface may not be aligned with the control surface hinge. As a result the control surface may overshoot and oscillation referred to as flutter can occur.
- **Actuation Issues** Hydraulic actuators are typically used to move the aerodynamic surfaces on a commercial aircraft. If hydraulic fluid leaks are present, the surface can be difficult to move.

Generally the actuator dynamics can be modelled by augmenting a second order transfer function $\frac{\omega_n^2}{s^2+2\zeta\omega_n+\omega_n^2}$ to each input channel with appropriate ω_n and ζ. Usually ζ is chosen to be 0.6 and ω_n depends on the high frequency roll of the nominal plant. However, in the case of the above model, the actuator dynamics and engine dynamics are added along with the state-space model, hence further augmentation is not performed. The 5th and 6th states of the model is related to actuator and engine dynamics.

2.3 Plant augmentation with integrator bank

Design Issues: Dynamic Augmentation In design problems, compensators with specific dynamics is required.

- It is known through *Internal Model Principle* that to follow step reference commands(in steady state), the compensator K must possess integrators within it. The compensator must have the form, $K = \frac{K_d}{s}$. Even if integrators are present within P, if input disturbance d_i are to be rjected (in steady state) then once again integrators are required within K.

For reasons stated above, it is often convenient to augment the plant $\mathbf{P} = \Big[A_p, B_p, C_p, D_p\Big]$ with desired dynamics (e.g. integrators). This is done solely for design purposes. These dynamics will ultimately be shifted into final compensator design. The resulting augmented plant is called a *Design Plant* and is denoted by $\mathbf{P_d} = \Big[A, B, C, D\Big]$ For our plant we would augment our plant $\mathbf{P}$ at its input with a bank of integrators $\frac{I_{m\times m}}{s}$, *i.e.* we would put one integrator per input channel. Since our model has $u \in \mathbb{R}^2$, there would be two new states added to our plant for the intergrators. The augmented system will be denoted by $P_d = \Big[A, B, C, D\Big]$ with inputs u, states $\Big[x_i^T x_p^T\Big]$ and output $y = y_p$. The state space representation for the following is:

$$\begin{bmatrix}\dot{x_p}\\ \dot{x_i}\end{bmatrix} = \begin{bmatrix}A_p & B_p\\ 0_{2\times 6} & 0_{2\times 2}\end{bmatrix}\begin{bmatrix}x_p\\ x_i\end{bmatrix} + \begin{bmatrix}0_{6\times 2}\\ I_{2\times 2}\end{bmatrix}\begin{bmatrix}\delta_s\\ \delta_t\end{bmatrix} \tag{6}$$

$$\begin{bmatrix}v\\ \gamma\end{bmatrix} = \begin{bmatrix}C_p & 0_{2\times 2}\end{bmatrix}\begin{bmatrix}x_p\\ x_i\end{bmatrix} \tag{7}$$

Design Procedure: Designing PK to obtain desirable closed loop properties

1. *Augment plant at input:* Augment the plant $\mathbf{P} = \Big[A_p, B_p, C_p, D_p\Big]$ at its input with desired dynamics, typically that of a integrator bank. This yields a design plant P_d as stated in (6) and (7). Note that this increases the order of the plant P.
2. *Design MBC Based on Design Plant P_d* Use the design plant $P_d = \Big[A, B, C, D\Big]$ to design a model based compensator
$$K_d = [\mathbf{A} - \mathbf{BG} - \mathbf{HC}, \mathbf{H}, \mathbf{G}] \tag{8}$$

where $\mathbf{D} = 0$. Due to this augmentation the associated $P_d K_d$ has desirable properties at plant output.**Note:** For the purpose of this project we choose **G** and **H** using design MIMO methodologies such as LQR, Kalman Filter, LQG, LQG/LTR,H_∞.

3. *Form final Compensator K* Form the final compensator K by absorbing the Integrator bank into K_d as follows:

$$K = \Big[A_k, B_k, C_k, D_k\Big] \tag{9}$$

where,

$$A_k = \begin{bmatrix} 0_{2\times 2} & \mathbf{G} \\ 0_{8\times 2} & \mathbf{A} - \mathbf{BG} - \mathbf{HC} \end{bmatrix},\ B_k = \begin{bmatrix} 0_{2\times 2} \\ \mathbf{H} \end{bmatrix} \tag{10}$$

$$C_k = \begin{bmatrix} I_{2\times 2} & 0_{2\times 8} \end{bmatrix} \tag{11}$$

Poles and Zeros. After augmentation our plant has two more states with the integrator poles. Following are the poles and zeros of the design plant.

$s_{1,2}$	$-1.2187 \pm 1.1672i$
$s_{3,4}$	$-0.0236 \pm 0.0975i$
s_5	$-12.0000 + 0.0000i$
s_6	$-1.9660 + 0.0000i$
$s_{7,8}$	$0.0000 + 0.0000i$
z_1	-6.8290
z_2	5.5464

The SVD plot of the plant after dynamic augmentation with integrators are as follows:
Similar set of steps can be followed to obtain desirable properties at the input. Next we will explore ways to obtain the **H** and **G** using the above stated design methodologies.

2.4 Bilinear Transformation

The plant has lightly damped stable phugoid modes at $s = 0.0236 \pm j0.0975(\zeta = 0.235, w_n = 0.1$ rads/sec). We use bilinear transformation to shift the lightly damped poles to the right half plane so that the controller obtained from any of the following design techniques like LQR,LQG,KBF and H_∞ does not cancel out the lightly damped poles. The following rules must be followed while selecting the parameters p_1 and p_2.

1. Parameter p_2 should be large ($p2 = -10^{20}$) so that the bilinear transformation merely becomes a rightward shifting transformation by p_1 units.
2. Parameter p_1 should be chosen in such a way that all poles which must not be canceled by the resulting controller should be moved into the right half plane after the bilinear transformation has been applied. Typically p_1 should be less than the minimum of the real parts of the plant poles which needs to be moved to the right half plane. In our problem, we require $p_1 < 0.0236$.
3. Parameter p_1 affects the bandwidth of the open loop and closed loop system. The bandwidth(open loop and closed loop) increases as p_1 is decreased(i.e. making it more negative).As bandwidth increases, the peak of the KS singular value plot increases i.e. more control action results for step commands. However, since AV-8A longitudinal dynamics has a RHP-zero which puts an upper bound on the acceptable bandwidth of the closed loop system, the selection of p_1 becomes critical. Therefore p_1 should not be made too negative.

The bilinear transformation parameters selected are as follows:

$$p_1 = -0.0944 \tag{12}$$

$$p_2 = -10^{20} \tag{13}$$

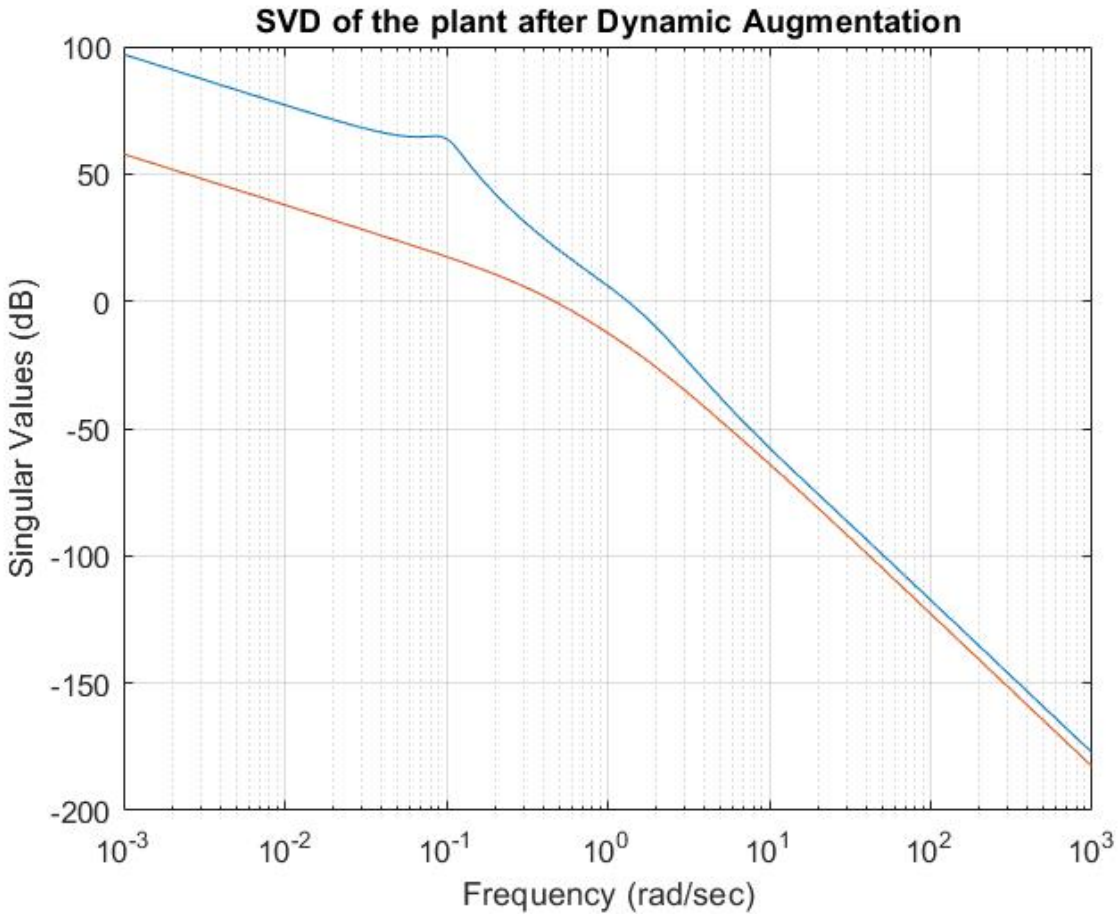

Figure 1: SVD of the plant after Dynamic Augmentation

The frequency response of the plant after bilinear transformation is in figure 2.
Disadvantage of Bilinear Transformation. The major disadvantage of bilinear transformation is the

Figure 2: SVD of the plant after Bilinear Transformation

loss of integral action, since after the inverse bilinear transformation, the integrator poles a $s = 0$ gets shifted slightly to the Left hand side of the imaginary axis.

3 Analysis of Model

3.1 Poles and Zeros

The aircraft has stable phugoid modes at $s = 0.0236 \pm j0.0975(\zeta = 0.235, w_n = 0.1$ rads/sec), stable short period modes at $s = 1.22 \pm j1.17(\zeta = 0.722, w_n = 1.69$ rads/sec). It has two damping modes at $s = -1.9660$ $s = -12.0000$ which comes due to the actuator dynamics and engine dynamics. It also has a transmission zero at $z = 5.5464$ and $z = 6.8290$. Following is the list of poles and zeros of the plant.

$s_{1,2}$	$-1.2187 \pm 1.1672i$
$s_{3,4}$	$-0.0236 \pm 0.0975i$
s_6	$-1.9660 + 0.0000i$
s_5	$-12.0000 + 0.0000i$
z_1	-6.8290
z_2	5.5464

Bandwidth Design Specification The presence of RHP-zero at $s = 5.5464$ makes designing a control system for AV-8A tedious because RHP-zero puts an upper bound on the acceptable closed loop bandwidth.Based on the presence of RHP-zero at $s = 5.5464$, we sought an open loop bandwidth of about $\omega_B^* < 0.5z$. The above condition is obtained from (Skogestad and Postlethwaite (2007) [2]. We choose an open loop bandwidth of about 1 rad/sec

3.2 System Transfer Functions: from u_i to y_j

The system transfer function matrix from u to y is given by:

$$\mathbf{G}(s) = \mathbf{C}(s\mathbf{I} - \mathbf{A}^{-1})\mathbf{B} + \mathbf{D} = \begin{bmatrix} \mathbf{G}_{\delta sv} & \mathbf{G}_{\delta tv} \\ \mathbf{G}_{\delta s\gamma} & \mathbf{G}_{\delta t\gamma} \end{bmatrix} \tag{14}$$

where,

$$\mathbf{G}_{\delta sv} = \frac{0.82749(s - 0.1078)(s^2 + 2.531s + 2.591)}{(s + 1.966)(s^2 + 0.0472s + 0.01007)(s^2 + 2.437s + 2.848)} \tag{15}$$

$$\mathbf{G}_{\delta v} = \frac{0.022529(s + 0.1154)(s^2 + 3.366s + 20.38)}{(s + 1.966)(s^2 + 0.0472s + 0.01007)(s^2 + 2.437s + 2.848)} \tag{16}$$

$$\mathbf{G}_{\delta s\gamma} = \frac{-0.5424(s + 10.62)(s - 8.763)(s + 0.48)}{(s + 12)(s^2 + 0.0472s + 0.01007)(s^2 + 2.437s + 2.848)} \tag{17}$$

$$\mathbf{G}_{\delta t\gamma} = \frac{1.1688(s + 6.753)(s - 5.458)(s + 0.02209)}{(s + 12)(s^2 + 0.0472s + 0.01007)(s^2 + 2.437s + 2.848)} \tag{18}$$

The individual transfer functions show the presence of stable phugoid modes at $s = 0.0236 \pm j0.0975$($\zeta = 0.235$,$w_n = 0.1$ rads/sec) and short period modes at $s = 1.22 \pm j1.17$($\zeta = 0.722$,$w_n = 1.69$ rads/sec). The transfer functions also show the presence of right half plane zeros at 5.5464.

3.3 Controllability and Observability

Definition 1 (**Controllability**). *A system is said to be controllable at $t = t_0$ if there exists a finite time $t_f > t_0$ such that for any initial state $x(t_0) = x_0$ and desired final state x_f, there exists a control $u(.)$ on $[t_0, t_f]$ that transfers the state of the system from $x(t_0) = x_0$ to $x(t_f) = x_f$. Otherwise the system is said to be uncontrollable. For an nth order LTI system (A,B,C,D) with m inputs the controllability matrix is as follows and if the rank $\mathcal{C}$ is equal to n, then the system is controllable:*

$$\mathcal{C} \triangleq \begin{bmatrix} \mathbf{B} & \mathbf{AB} & \cdots & \mathbf{A}^{n-1}\mathbf{B} \end{bmatrix} \tag{19}$$

For our system, the $\mathcal{C}$ matrix is:

$$\mathcal{C} = \begin{bmatrix} \mathbf{B} & \mathbf{AB} & \mathbf{A}^2\mathbf{B} & \mathbf{A}^3\mathbf{B} \end{bmatrix} \tag{20}$$

The rank of our $\mathcal{C}$ is **6**, therefore our system is controllable.

Definition 2 (**Observability**). *A system is said to be observable at $t = t_0$ if there exists a finite time $t_f > t_0$ such that the initial condition $x(t_0) = x_0$ can be uniquely determined given knowledge of the input $u(.)$ and the output $y(.)$on $[t_0, t_f]$. Otherwise the system is said to be unobservable. For an nth order LTI system (A,B,C,D) with m inputs the observability matrix is as follows and if the rank $\mathcal{C}$ is equal to n, then the system is observable:*

$$\mathcal{O} \triangleq \begin{bmatrix} \mathbf{C} \\ \mathbf{CA} \\ \vdots \\ \mathbf{CA}^{n-1} \end{bmatrix} \tag{21}$$

For our system, the $\mathcal{O}$ matrix is:

$$\mathcal{O} = \begin{bmatrix} \mathbf{C} \\ \mathbf{CA} \\ \mathbf{CA}^2 \\ \mathbf{CA}^3 \end{bmatrix} \tag{22}$$

The rank of our $\mathcal{O}$ is **6**, therefore our system is observable.

3.4 Modal Analysis

The aircraft has stable phugoid modes at $s = 0.0236 \pm j0.0975(\zeta = 0.235, w_n = 0.1$ rads/sec), stable short period modes at $s = 1.22 \pm j1.17(\zeta = 0.722, w_n = 1.69$ rads/sec).

- *Stable phugoid mode:* The system exhibits stable very lightly damped oscillatory mode. at $s = 0.0236 \pm j0.0975(\zeta = 0.235, w_n = 0.1$ rads/sec). The eigenvector for the mode is as follows:

$v_{1,2}$	$0.0012 \pm 0.0030i$
$v_{3,4}$	$-0.0003 \pm 0.0000i$
$v_{5,6}$	$0.0006 \pm 0.0031i$
$v_{7,8}$	$-1.0000 \pm 0.0000i$
$v_{9,10}$	$0.0000 \pm 0.0000i$
$v_{11,12}$	$0.0000 \pm 0.0000i$

  The associated right eigenvector shows that this mode is primarily associated with v and an almost constant q. The mode involved a continuous rise and fall of teh aircraft with potential and kinetic energy being exchanged. This mode has a very high time constant $\tau = 42$ sec. The visualization of the following mode is in displayed in fig 3.

- *Short stable mode:* The system exhitbits damped short mode at $s = 1.22 \pm j1.17(\zeta = 0.722, w_n = 1.69$ rads/sec). The eigenvector is for the following mode is as follows:

$v_{1,2}$	$0.0322 \pm 0.0340i$
$v_{3,4}$	$0.0004 \pm 0.0790i$
$v_{5,6}$	$-0.0176 \pm 0.0047i$
$v_{7,8}$	$0.9956 \pm 0.0000i$
$v_{9,10}$	$0.0000 \pm 0.0000i$
$v_{11,12}$	$0.0000 \pm 0.0000i$

  The associated right eigenvector shows that this mode is primarily associated with velocity direction primarily the angle of attack. This is a very fast mode with $\tau = 0.81$ sec. The motion is a rapid pitching of the aircraft about the center of gravity. The period is so short that the speed does not have time to change, so the oscillation is essentially an angle-of-attack variation [3]. The visualization of the following mode is in displayed in fig 4.

- *Damping Modes* The damping modes are associated with actuator dynamics and engine dynamics for the 5th and 6th states.

3.5 Frequency Response

MIMO Frequency Response: Singular Values The MIMO singular values for the plant transfer matrix from controls $u = \left[\delta_s, \delta_t\right]$ to plant output $y = \left[\text{FPA,Vel}\right]$ are plotted in Figure5. The plot shows a peaking at 0.1 rads/sec due to the lightly damped phugoid mode at at $s = 0.0236 \pm j0.0975(\zeta = 0.235, w_n = 0.1$ rads/sec).

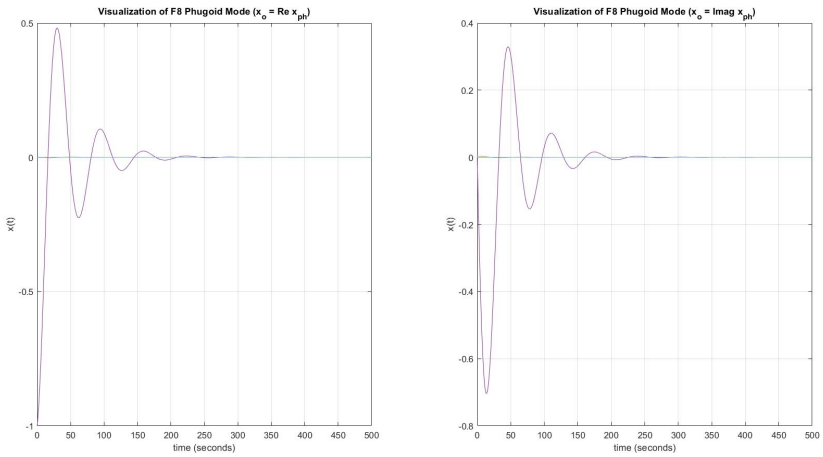

Figure 3: AV-8A Harrier Phugoid Mode Time Response

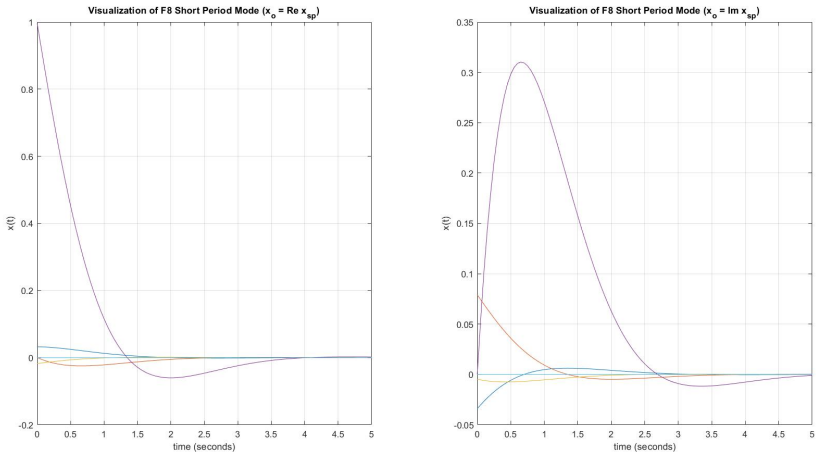

Figure 4: AV-8A Harrier Short Mode Time Response

In the plot, we notice that the minimum singular values of the plant corresponding to the δ_s channel channel are low and wide spread at low frequencies. Hence the resulting controller will have to compensate for the low plant gain in the δ_s channel. Thus we expect that significant stick input activity will be required in order to achieve a loop with desirable low frequency disturbance attenuation(e.g. $\sigma_{min}[PK] > 20$ db at low frequencies) and desirable low frequency command following.

DC Gain Analysis using Singular Value Decomposition While analyzing the AV-8A Harrier model at DC, we get the following matrix of DC gains:

$$\begin{bmatrix} v \\ \gamma \end{bmatrix} = \begin{bmatrix} -4.0996 & 70.4110 \\ 0.9400 & -2.7658 \end{bmatrix} \begin{bmatrix} \delta_s \\ \delta_t \end{bmatrix} \tag{23}$$

A singular value decomposition at DC yields the following:

$$\mathbf{G}(j0) = \mathbf{C}(-\mathbf{A}^{-1})\mathbf{B} + \mathbf{D} = \mathbf{U}\mathbf{\Sigma}\mathbf{V}^{\mathbf{T}} \tag{24}$$

where,

$$U = \begin{bmatrix} 0.9992 & -0.0399 \\ -0.0399 & -0.9992 \end{bmatrix} \Sigma = \begin{bmatrix} 70.5864 & 0 \\ 0 & 0.7770 \end{bmatrix} V = \begin{bmatrix} -0.0586 & -0.9983 \\ 0.9983 & -0.0586 \end{bmatrix} \tag{25}$$

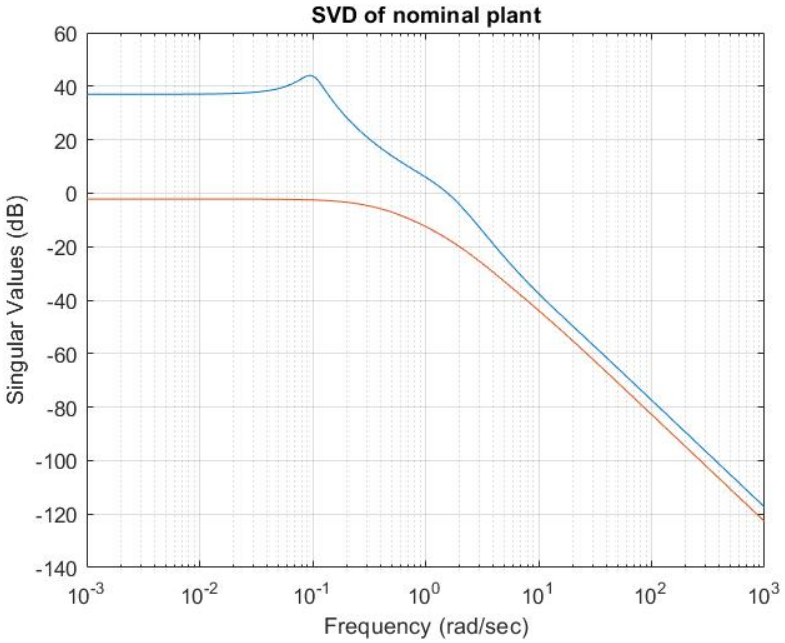

Figure 5: AV-8A Harrier Longitudinal Dynamics Singular Values MIMO Frequency Response

The relation between the right and left singular values gives an idea of how the input and output are coupled. This would also corroborate our assumption that during simplification and operating the flight at medium speed condition we were able to decouple the inputs and outputs. The following figure 6 shows the relation between the $v \rightarrow \sigma u$.

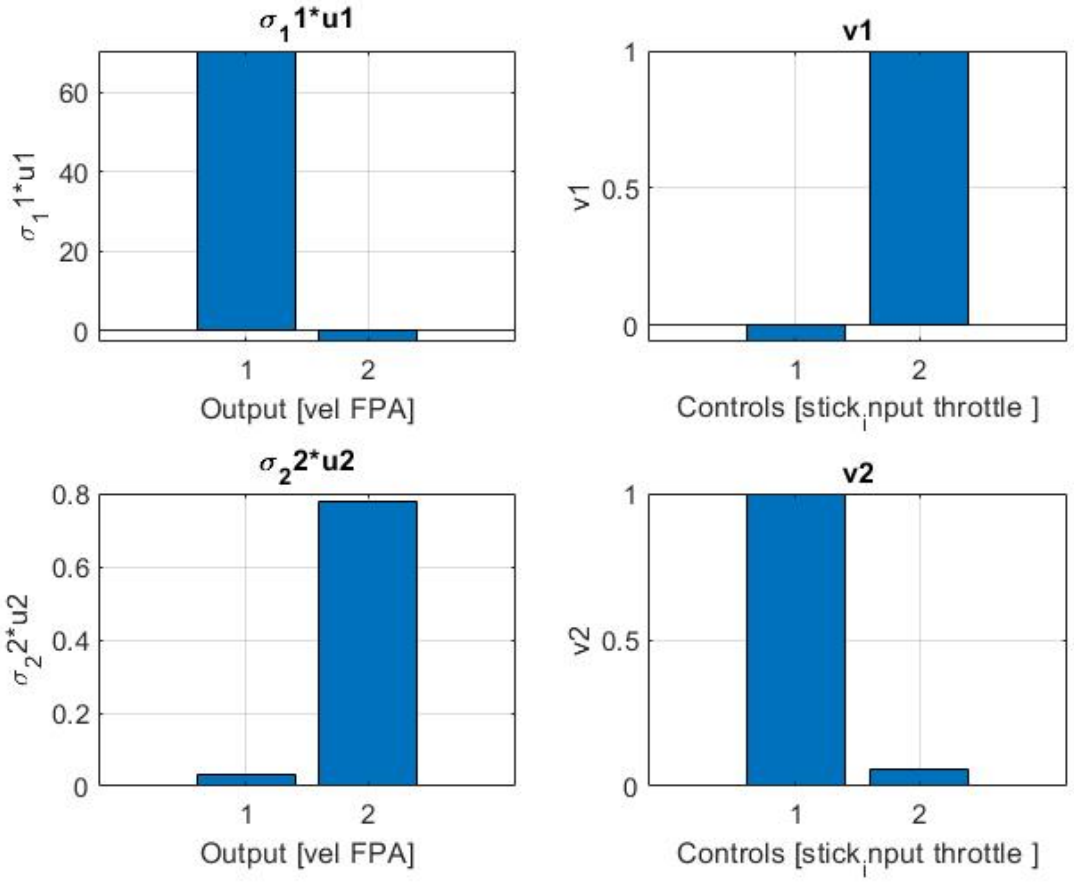

Figure 6: AV-8A Harrier SVD at DC for Longitudinal Dynamics

1. Examination of the first columns of V,Σ and U shows that throttle has a greater impact on the velocity of the aircraft compared to the flight path angle .This may be visualized as shown in Figure 6. This analysis shows that throttle should be used as the primary control for maintaining steady velocity perturbations from equilibrium.

2. It also shows that that stick input has a greater impact stick input on the flight path angle of the aircraft than the velocity of the aircraft. This may be visualized as shown in Figure 6. This analysis shows that stick input should be used as the primary control for maintaining steady flight path angle perturbations from equilibrium.

The Singular Value Decomposition at DC shows that AV8A longitudinal dynamics is sufficiently decoupled at DC. Below are the singular value decomposition for phugoid mode at $s = j * 0.0975$ and short mode at $s = j * 1.1672$

$$U = \begin{bmatrix} \text{-0.5913 - 0.7879i} & \text{-0.0294 + 0.1694i} \\ \text{-0.0830 + 0.1505i} & \text{-0.9542 + 0.2449i} \end{bmatrix} \Sigma = \begin{bmatrix} 158.8461 & 0 \\ 0 & 0.7489 \end{bmatrix} \tag{26}$$

$$V = \begin{bmatrix} \text{-0.0772 + 0.0000i} & \text{-0.9970 + 0.0000i} \\ \text{0.6413 - 0.7634i} & \text{-0.0497 + 0.0591i} \end{bmatrix} \tag{27}$$

$$U = \begin{bmatrix} \text{0.1471 + 0.7756i} & \text{0.3068 + 0.5316}i \\ \text{0.1101 - 0.6038i} & \text{0.1225 + 0.7799i} \end{bmatrix} \Sigma = \begin{bmatrix} 1.6055 & 0 \\ 0 & 0.2001 \end{bmatrix} \tag{28}$$

$$V = \begin{bmatrix} \text{-0.1542 + 0.0000i} & \text{-0.9880 + 0.0000i} \\ \text{-0.1907 - 0.9695i} & \text{0.0298 + 0.1513i} \end{bmatrix} \tag{29}$$

4 Control Design

4.1 Linear Quadratic Regulator (LQR) Design

Pole placement can be a good strategy for stabilizing feedback systems, but its more effective for SISO. In MIMO systems, its more effective to use a LQR theory to determine the placement of the closed loop poles to ensure good full state feedback control laws that offer nominal stability and good robustness properties.

- **Plant Model** The MIMO LTI model is defined after dynamic augmentation and bilinear transformation as:

$$\dot{x} = \mathbf{A}x + \mathbf{B}u \qquad\qquad x(0) = x_o \tag{30}$$

  The immediate goal is to formulate an optimization problem that would result in a state feedback control law $u = -\mathbf{G}x$ that will drive the initial condition to zero.

- **Quadratic Cost** The quadratic cost that needs to be minimized to get the optimal solution is defined by

$$J(u) \triangleq \frac{1}{2}\int_0^\infty (x^T\mathbf{Q}x + u^T\mathbf{R}u)d\tau \tag{31}$$

- For our system, we are taking state weighting matrix $\mathbf{Q} = \mathbf{C^T C}$. The above $\mathbf{Q}$ penalizes the states which directly contributes to the output y. Namely, for our case the states of velocity and FPA are equally penalized. For better control, these weights can be adjusted to achieve even better frequency response and CLS properties.

- The control weighting matrix $\mathbf{R} = 1.0e-9 * \mathbf{I_{2\times 2}}$. We are going for cheaper control hence we are taking a small ρ. Also due to the presence of a RHP zero in AV-8A Harrier, there is a limit to the Bandwidth, hence we cannot arbitrarily increase(decrease) ρ.

- The G and K matrices after Algebraic Riccati equation is as follows:

$$G = \begin{bmatrix} -0.1348 & -0.0142 & -0.1685 & 0.0312 & 0.0008 & -0.0000 & 0.0001 & -0.0000 \\ -0.3480 & -0.0603 & -1.4586 & -0.0045 & -0.0001 & 0.0002 & -0.0000 & 0.0001 \end{bmatrix} \times 1.0e+06 \tag{32}$$

$$K = \begin{bmatrix} 0.0164 & 0.0025 & 0.1254 & -0.0002 & -0.0000 & -0.0000 & -0.0000 & -0.0000 \\ 0.0025 & 0.0004 & 0.0187 & -0.0000 & -0.0000 & -0.0000 & -0.0000 & -0.0000 \\ 0.1254 & 0.0187 & 1.1273 & -0.0009 & -0.0000 & -0.0000 & -0.0000 & -0.0000 \\ -0.0002 & -0.0000 & -0.0009 & 0.0001 & 0.0000 & -0.0000 & 0.0000 & -0.0000 \\ -0.0000 & -0.0000 & -0.0000 & 0.0000 & 0.0000 & -0.0000 & 0.0000 & -0.0000 \\ -0.0000 & -0.0000 & -0.0000 & -0.0000 & -0.0000 & 0.0000 & -0.0000 & 0.0000 \\ -0.0000 & -0.0000 & -0.0000 & 0.0000 & 0.0000 & -0.0000 & 0.0000 & -0.0000 \\ -0.0000 & -0.0000 & -0.0000 & -0.0000 & -0.0000 & 0.0000 & -0.0000 & 0.0000 \end{bmatrix} \tag{33}$$

Open Loop and Closed loop properties The resulting closed loop system is defined as

$$\dot{x} = (\mathbf{A} - \mathbf{BG})x \tag{34}$$

The open loop LQR transfer function matrices are as follows:

$$G_{OL} \triangleq \mathbf{M}(sI - \mathbf{A})^{-1}\mathbf{B} \tag{35}$$

$$G_{LQ} \triangleq \mathbf{G}(sI - \mathbf{A})^{-1}\mathbf{B} \tag{36}$$

G_{LQ} after inverse bilinear transfer function has the following transfer functions:

- From input 1 to output ...
  1. $\frac{56.906(s-0.1139)(s^2+2.515s+2.547)(s^2+30.53s+451.9)}{s(s+1.966)(s^2+0.0472s+0.01007)(s^2+2.437s+2.848)}$
  2. $\frac{-1.9213(s+0.03183)(s^2+3.105s+4.637)(s^2+89.62s+2552)}{s(s+1.966)(s^2+0.0472s+0.01007)(s^2+2.437s+2.848)}$
- From input 2 to output ...
  1. $\frac{-1.9213(s-37.76)(s+11.34)(s+0.443)(s^2+75.52s+2095)}{s(s+12)(s^2+0.0472s+0.01007)(s^2+2.437s+2.848)}$
  2. $\frac{66.471(s+8.367)(s+3.59)(s-0.05708)(s^2+35.85s+601.3)}{s(s+12)(s^2+0.0472s+0.01007)(s^2+2.437s+2.848)}$

The Sensitivity and the complementary sensitivity matrices are defined as follows:

$$S_{LQ} \triangleq \Big[I + G_{LQ}\Big]^{-1} \tag{37}$$

$$T_{LQ} \triangleq \Big[I + G_{LQ}\Big]^{-1} G_{LQ} \tag{38}$$

$$\tag{39}$$

The resulting closed loop Sensitivity and Complementary Sensitivity plots are in figure 7 and 8.

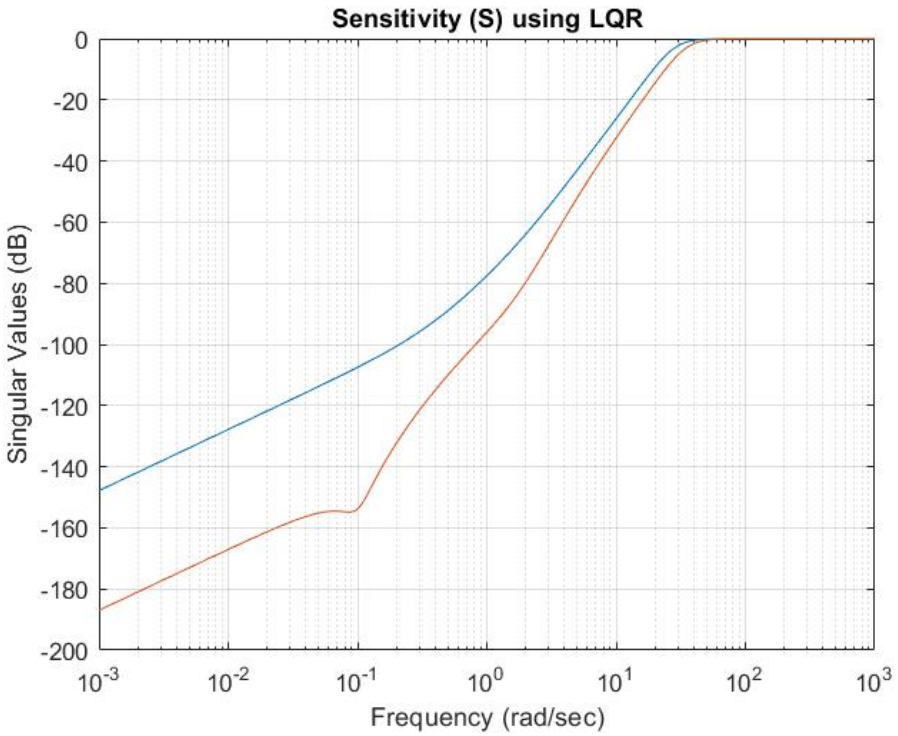

Figure 7: SVD of the Sensitivity using LQG

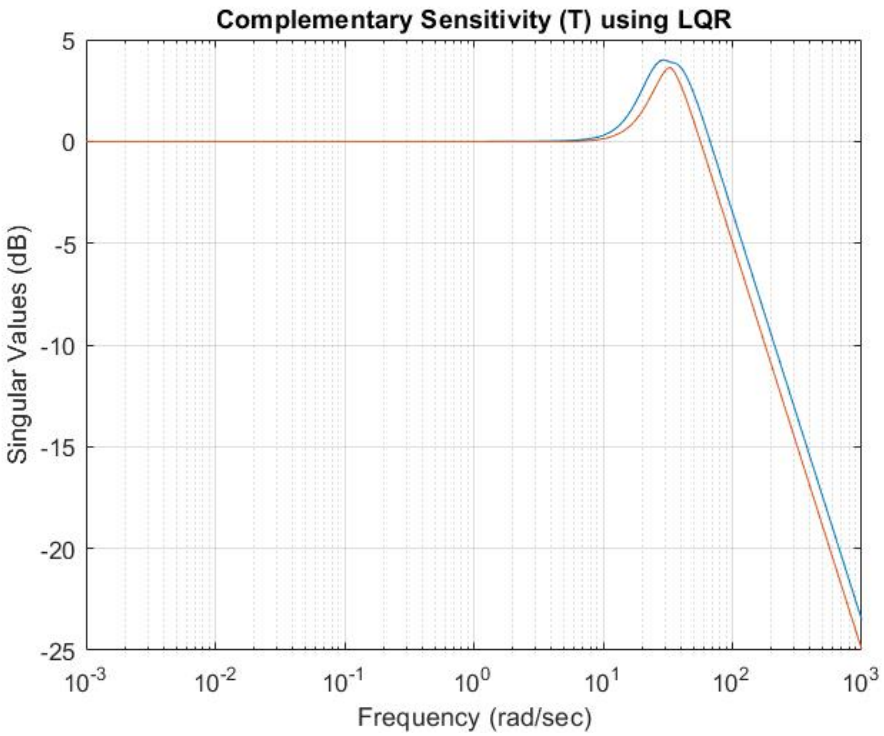

Figure 8: SVD of the Complementary Sensitivity using LQG

The concept of LQR is used to determine the control gain matrix G for the LQG and LTRO design methodology as well. There we see how exactly the closed loop poles are placed and all the open loop and closed loop properties are analysed in the subsequent sections.

4.2 Kalman Filter

Pole-placement can used to design state/observer estimators for SISO system, It is however not effective for MIMO systems.

- **System Dynamics**. We begin by considering the LTI MIMO system to have the following model:

$$\dot{x} = \mathbf{A}x + \mathbf{B}u + \mathbf{L}\zeta \qquad x(t_o) = x_o \tag{40}$$

$$y = \mathbf{C}x + \mathbf{D}u + \theta \tag{41}$$

- **Initial Condition**. x_o is an uncertain initial condition. Only apriori first and second order statistics are assumed to be available.

$$\mathbb{E}((x_o - m_o)(x_o - m_o)^T) = \Sigma_o \qquad \Sigma_o = \Sigma_o^T \geq 0 \tag{42}$$

- **Process Noise** ζ is called process noise. Its assumed to be a WSS stochastic process.
- **Measurement Noise** θ is the measurement noise or sensor noise. It is also assumed to be a WSS stochastic process. Only a priori first and second order statistics are considered here.
- **Goal** We develop a state estimation structure from the initial condition, process noise and measurement noise. The State estimation error is defined as:

$$\dot{x} \triangleq x - \hat{x} \tag{43}$$

- The process noise matrix is chosen to be $I_{2\times 2}$ and the measurement noise matrix is chosen to be $diag(0.1, 0.1)$. These measurements can be further modified to obtain better observer estimation.
- The resulting H matrix from MATLAB kalman command is as follows:

$$\mathbf{H} = \begin{bmatrix} -0.0995 & 0.1104 \\ -0.0862 & 0.0776 \\ -0.0189 & 0.0316 \\ 2.5790 & -1.0820 \\ 1.8760 & 2.3124 \\ 2.4105 & -2.0563 \\ 2.0549 & 2.4119 \\ 2.4101 & -2.0544 \end{bmatrix} \tag{44}$$

The **H** matrix is used in LQG and LTRO design methodology to get the observer gain matrix. The open and close loop analysis are explored in subsequent sections.

4.3 Linear Quadratic Gaussian (LQG) Design

The linear quadratic Gaussian (LQG) control problem is one of the most fundamental optimal control problems. It concerns linear systems driven by additive white Gaussian noise. The problem is to determine an output feedback law that is optimal in the sense of minimizing the expected value of a quadratic cost criterion. This control law which is known as the LQG controller, is unique and it is simply a combination of a Kalman filter (a linearquadratic state estimator (LQE)) together with a linearquadratic regulator (LQR). The separation principle states that the state estimator and the state feedback can be designed independently.LQG optimality does not automatically ensure good robustness properties. The robust stability of the closed loop system must be checked separately after the LQG controller has been designed. To promote robustness some of the system parameters may be assumed stochastic instead of deterministic. Here in our design we explore the idea of using LQG for systems such as these. To further induce good properties, the selection of weights of both **G** and **H** matrices needs to be further improved and optimized.

- LQG can be viewed as a combination of LQR and Kalman filter, where **G** and **K** matrices are obtained from LQR and **H** and Σ matrices are obtained from Kalman filter
- The LTI system is first described by the equation:

$$\dot{x} = \mathbf{A}x + \mathbf{B}u + \mathbf{L}\zeta \tag{45}$$
$$y = \mathbf{C}x + \Theta \tag{46}$$
$$\tag{47}$$

  Here the LQR contributes to **A** and **B** of the plant and **L**,**C** and Θ comes from the Kalman filter.

- Based on these $P = \Big[\mathbf{A}, \mathbf{B}, \mathbf{C}\Big]$ is formed and a Model-Based-Compensator (K_{MBC}) is developed.

$$K_{MBC} = [\mathbf{A} - \mathbf{BG} - \mathbf{HC}, -\mathbf{H}, -\mathbf{G}] \tag{48}$$

- The final compensator is formed after augmenting the the K_{MBC} with the integrators. Here, we are using the `f_CLFTM.m` function to generate the open loop and closed frequency plots.
- The **G** and **H** matrices are selected as follows:

$$\mathbf{G} = \begin{bmatrix} -0.2959 & -0.0364 & -0.7670 & 0.0981 & 0.0009 & -0.0000 & 0.0000 & -0.0000 \\ -1.0096 & -0.1570 & -4.6705 & -0.0184 & -0.0001 & 0.0002 & -0.0000 & 0.0000 \end{bmatrix} \times 1.0e+07 \tag{49}$$

$$\mathbf{H} = \begin{bmatrix} -0.0995 & 0.1104 \\ -0.0862 & 0.0776 \\ -0.0189 & 0.0316 \\ 2.5790 & -1.0820 \\ 1.8760 & 2.3124 \\ 2.4105 & -2.0563 \\ 2.0549 & 2.4119 \\ 2.4101 & -2.0544 \end{bmatrix} \tag{50}$$

- The Nominal CLS will be stable but there are no guaranteed robustness properties.
- Better design can be obtained by using LQG/LTR method for our system.

Open Loop Analysis Breaking the loop at e or y yields the open loop transfer function matrix $\mathbf{L}_e = \mathbf{PK}$. Its singular values are plotted at figure 9. The singular values are matched at low frequencies with a slope of -20dB/dec due to integral action at each input control channel. The plot suggest that low frequency reference command r will be followed, low frequency output disturbance d_o will be attenuated and high frequency noise will be attenuated. Breaking the loop at input u yields the open loop transfer function matrix $L_u = \mathbf{KP}$. It

must be emphasized that $\mathbf{KP} \neq \mathbf{PK}$ since matrix multiplication doesnt commute. The associated transfer function matrix is

$$T_{d_i u_p} = \Big[I + \mathbf{KP}\Big]^{-1} = \Big[I + L_u\Big]^{-1} \tag{51}$$

The singular values suggests that input disturbances d_i with frequency content below 0.1 rad/sec will be attenuated by about 20 dB/dec - resulting in a u_p having about one-tenth of the disturbance. Large wiggles in u_p may result in actuator degradation or premature failure. The plot of singular values is shown in figure 10

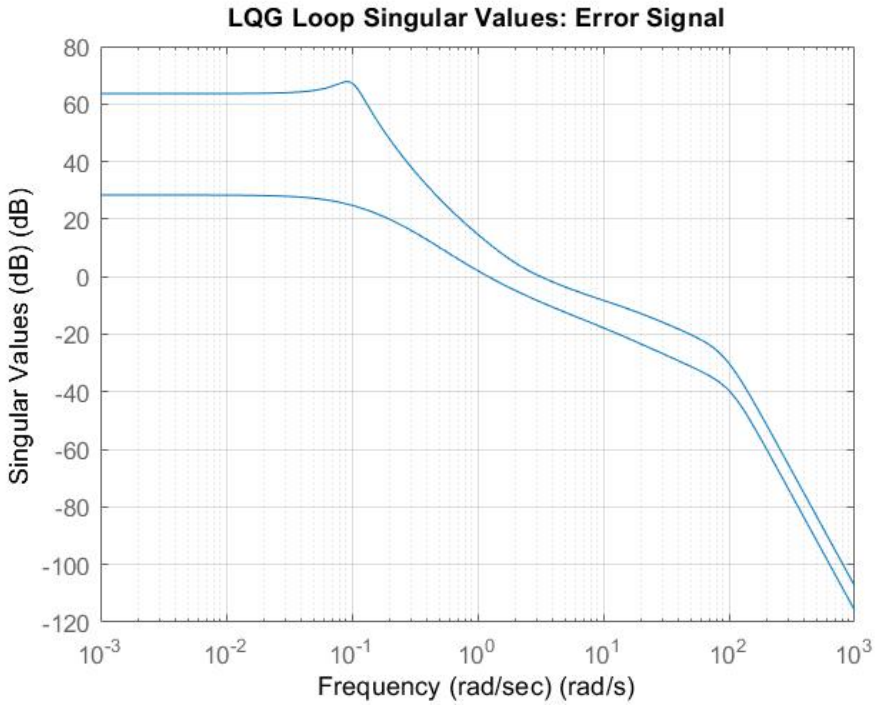

Figure 9: SVD of the Open loop error using LQG

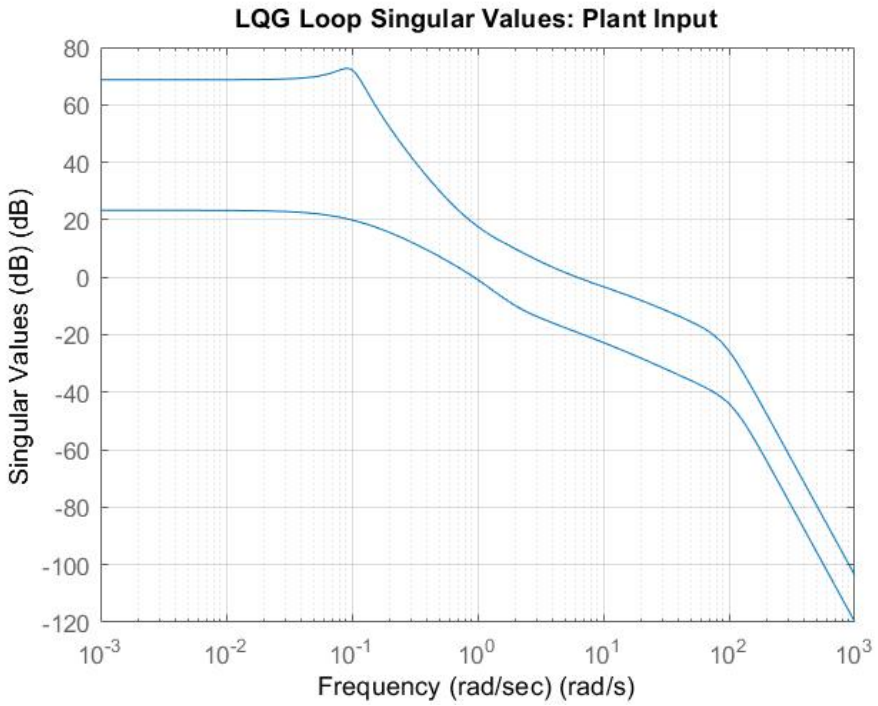

Figure 10: SVD of the Open Loop Error using LQG

Closed Loop Analysis Sensitivity Frequency Response at error. The sensitivity transfer function matrix associated with e is given by:

$$S_e = \Big[I + \mathbf{PK}\Big]^{-1} = \Big[I + L_e\Big]^{-1} \tag{52}$$

We can see from figure 11 and10 that the values of sensitivity is below -10 dB at low frequencies and that peak values of sensitivity is below 3 dB at input. This ensures that the systems has good robust margins for small gain conditions. Also this signifies that the design has good low frequency command following and good low frequency disturbance attenuation at both input and output of the plant. Since there is RHP-zero present in the system, we cannot indiscriminately push the sensitivity at low frequency as the resulting popping of the sensitivity at higher frequency would not satisfy the bandwidth criteria of the system. The peak of the sensitivity matrix is also important and is associated with near-imaginary axis poles of the resulting closed loop system, which is undesirable. However, the peak sensitivity could not be reduced further for the above mentioned BW consideration. The peak sensitivity is bounded by α. Our design here has a peak sensitivity less that 5.08 dB. This is due to the fact we are restricted by overall bandwidth of the nominal plant. The contraint is mainly due to RHP-zero. Better design can be achieved by selecting the weights of Q and R with further experiments.

Complementary Sensitivity Frequency Response at Output. The complementary sensitivity frequency response at output or e is given by:

$$T_e = I - S_e = \mathbf{PK}\Big[I + \mathbf{PK}\Big]^{-1} \tag{53}$$

These effective closed loop properties come from the fact that the weighting function for the H_∞ has been chosen according to the ideal conditions for sensitivity and complementary sensitivity. The complementary sensitivity graph from figure 14 and 13 shows that the system has good high frequency noise attenuation. There is -50 dB noise attenuation after 5.54 rad/sec. The K-Sensitivity graph shows how much additive uncertainty can be tolerated by the system. Since our KS is stable, the closed loop system will be stable for all stable additive perturbations Δ_a.

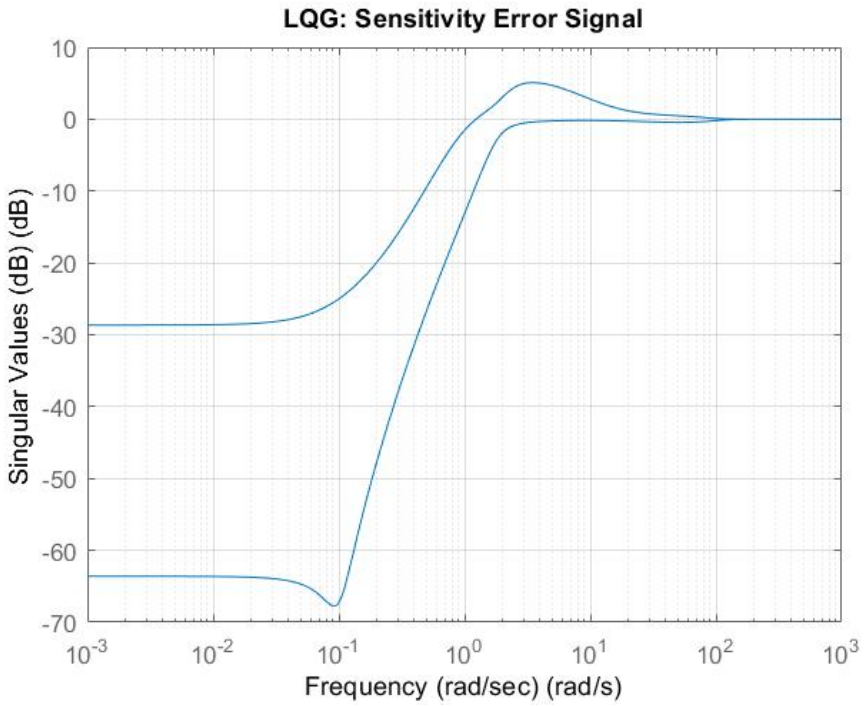

Figure 11: SVD of the Sensitivity at error using LQG

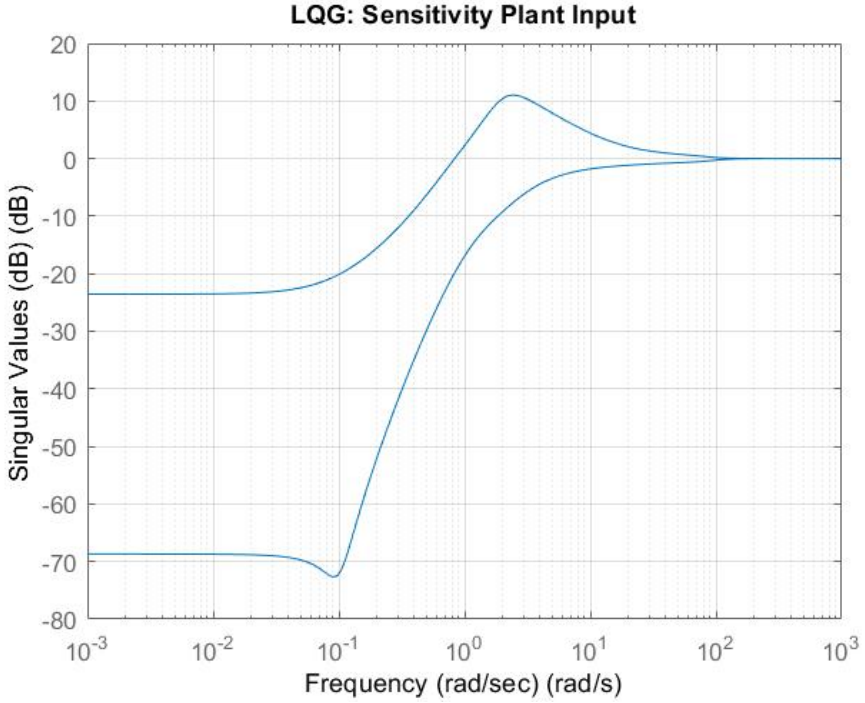

Figure 12: SVD of the Sensitivity at input using LQG

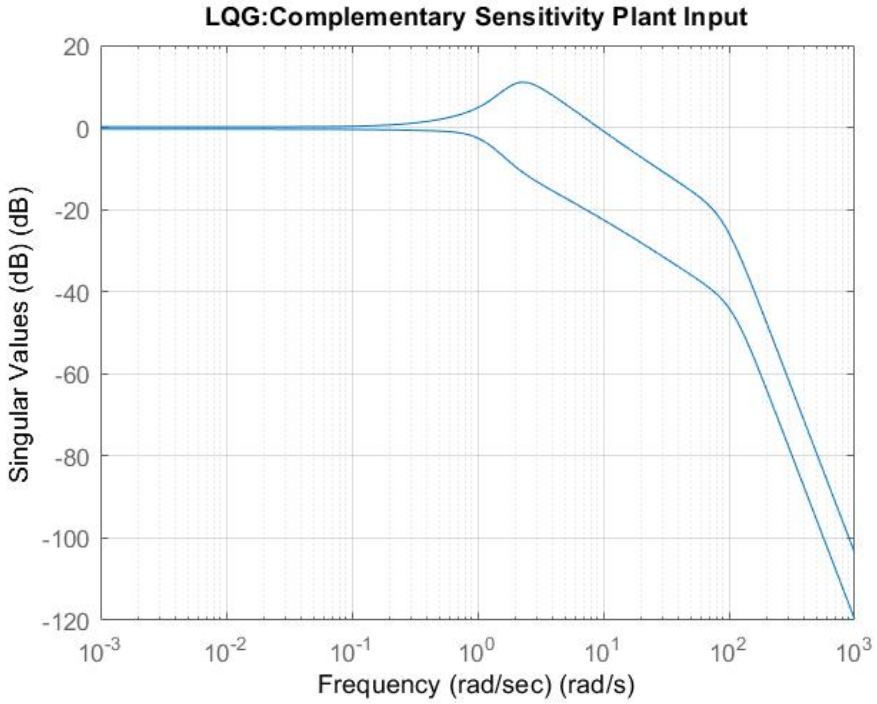

Figure 13: SVD of the Complementary Sensitivity at input using LQG

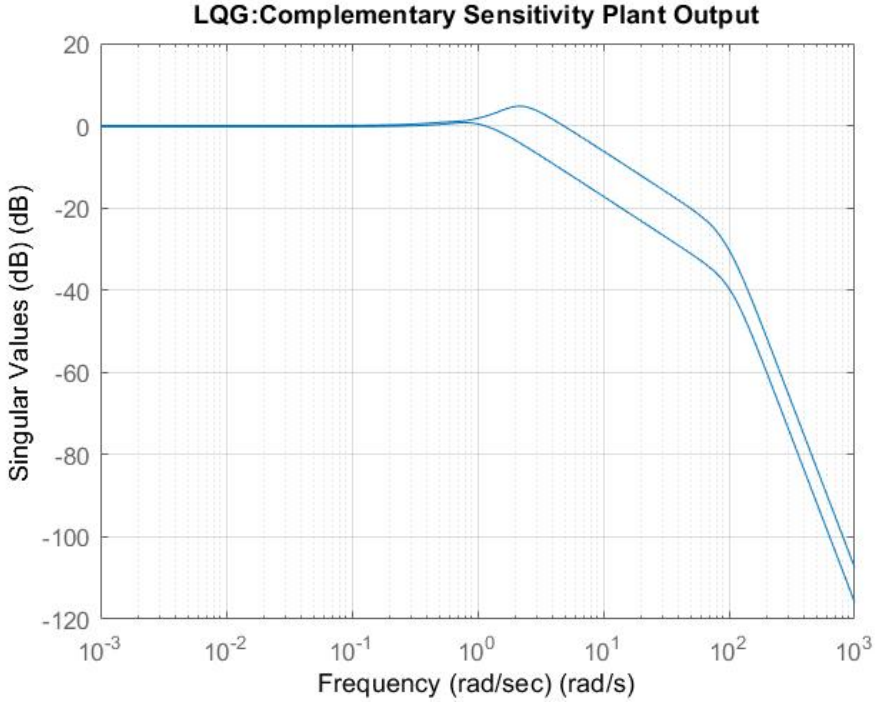

Figure 14: SVD of the Complementary Sensitivity at output using LQG

Time Domain Analysis The Time domain analysis shows that the the system after LQG design has good command following step responses to both Velocity and FPA. Here the importance is given to reduce the settling time and the overshoot is relaxed. The overshoot can also be reduced using a pre-filter which will cancel the zeros which gets introduced in the controller. The visualization for the time domain analysis is shown in figure 15. Here better response can be obtained in LQG/LTR method.

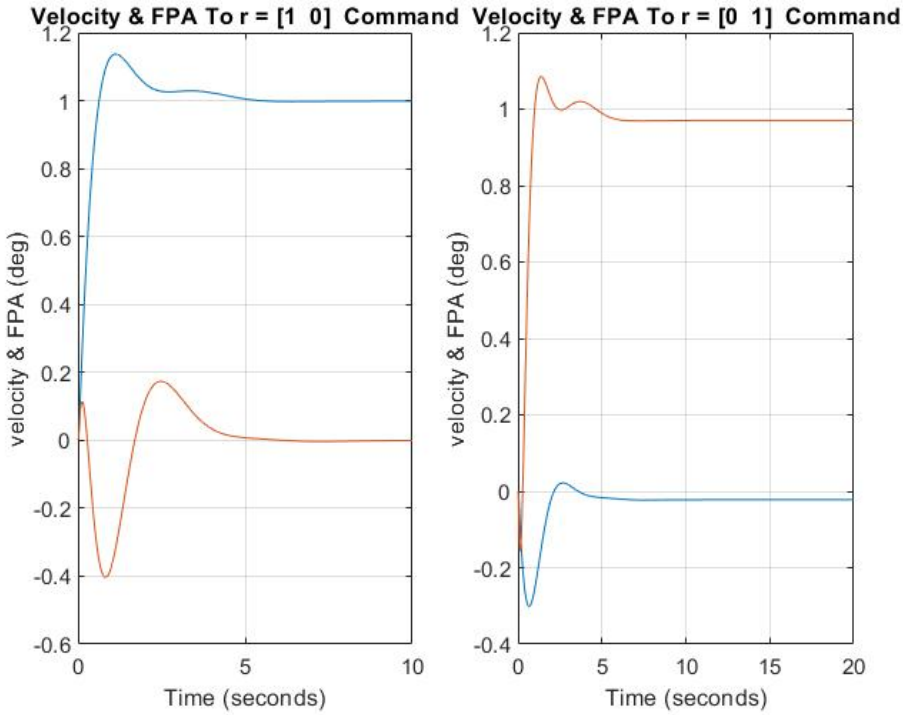

Figure 15: Time Response of Velocity and FPA using LQG

4.4 LQG/Loop Transfer Recovery (LTR) Design

To recover good output properties, Loop Transfer Recover at Output is performed, then after the target is set by Kalman filter ideas, LQG controller is then used to obtain desired controller. The process ensures the controller has closed loop stability, zero steady state error to step reference, good low frequency command following, good low frequency disturbance attenuation, good high frequency noise attenuation and good stability robustness margins.

- The plant is first augmented with integrators as described in previous section.
- Then the Target loop transfer function matrix is obtained

$$L_o = \mathbf{G}_{KF} = \mathbf{C}(sI - \mathbf{A})^{-1}\mathbf{H} \tag{54}$$

  Like LQR loops designed without a cross state control coupling penalty, KF loops designed in similar fashion to exhibit desirable stability robustness margins. The target open loop is carried in the following way:

$$L = \begin{bmatrix} L_L \\ L_H \end{bmatrix} \tag{55}$$

$$L_L = \left[\mathbf{C}_p(-\mathbf{A}_p)^{-1}\mathbf{B}_p\right]^{-1} \tag{56}$$

$$L_H = (-\mathbf{A}_p)^{-1}\mathbf{B}_p\mathbf{L}_L \tag{57}$$

  The matrix L_L matches the singular values of $G_{FOL} = \mathbf{C}(sI - \mathbf{A})^{-1}\mathbf{L}$ at low frequencies. The matrix L_H matches the singular values at high frequencies. Together they recover the target at all frequencies. The visualization for the target loops are provided in figure 16,17,18 and 19.

- The $\mathbf{G}$ and $\mathbf{H}$ matrix are as follows:

$$\mathbf{G} = \begin{bmatrix} -0.1348 & -0.0142 & -0.1685 & 0.0312 & 0.0008 - 0.0000 & 0.0001 & -0.0000 \\ -0.3480 & -0.0603 & -1.4586 & -0.0045 & -0.0001 & 0.0002 & -0.00000.0001 \end{bmatrix} \times 1.0e+06 \tag{58}$$

$$\mathbf{H} = \begin{bmatrix} -0.0038 & 0.0529 \\ 0.0000 & -0.0000 \\ -0.0000 & 0.0552 \\ 3.1633 & -0.0000 \\ 0.1595 & 4.0611 \\ 0.0542 & 0.2365 \\ 0.1595 & 4.0611 \\ 0.0542 & 0.2365 \end{bmatrix} \tag{59}$$

- The final controller K is constructed in the same way as described above.Here, we are using the `f_CLFTM.m` function to generate the open loop and closed frequency plots.

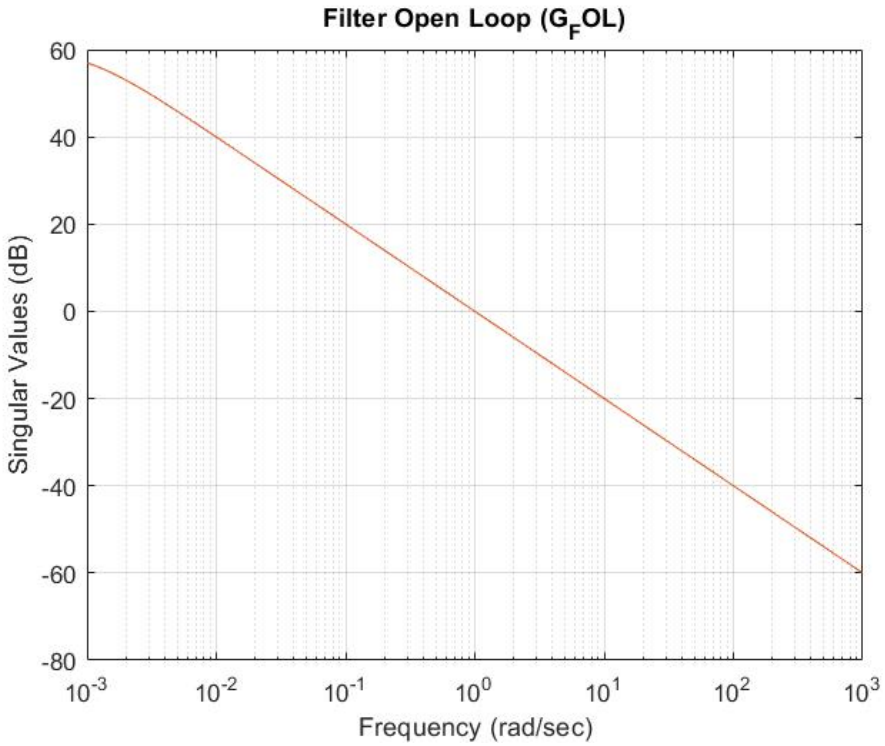

Figure 16: SVD of the LTR G_{FoL}

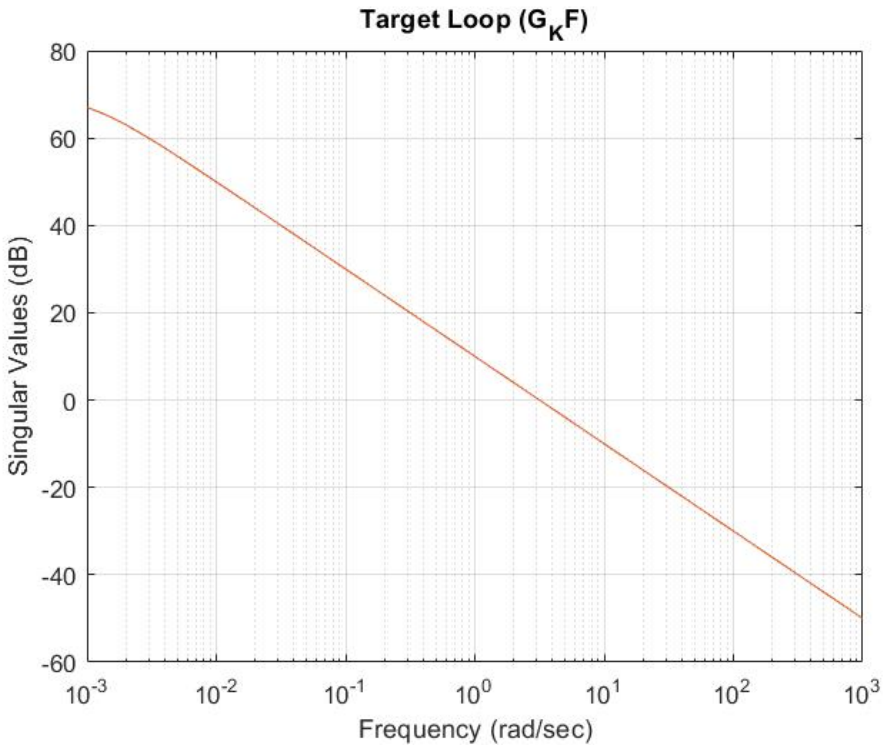

Figure 17: SVD of the LTR G_{KF}

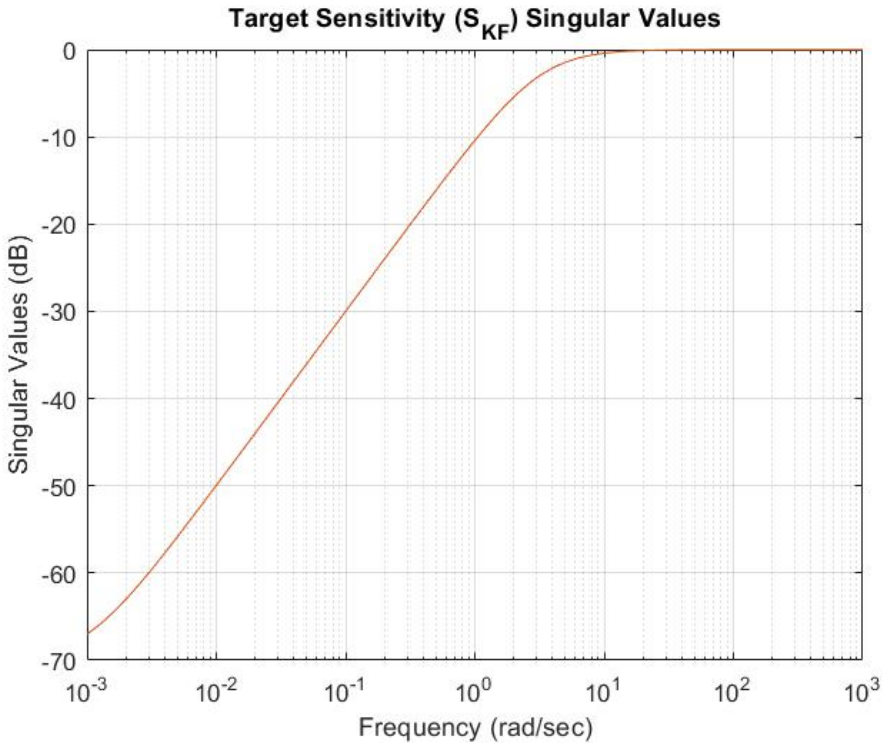

Figure 18: SVD of the Target Sensitivity using LTR

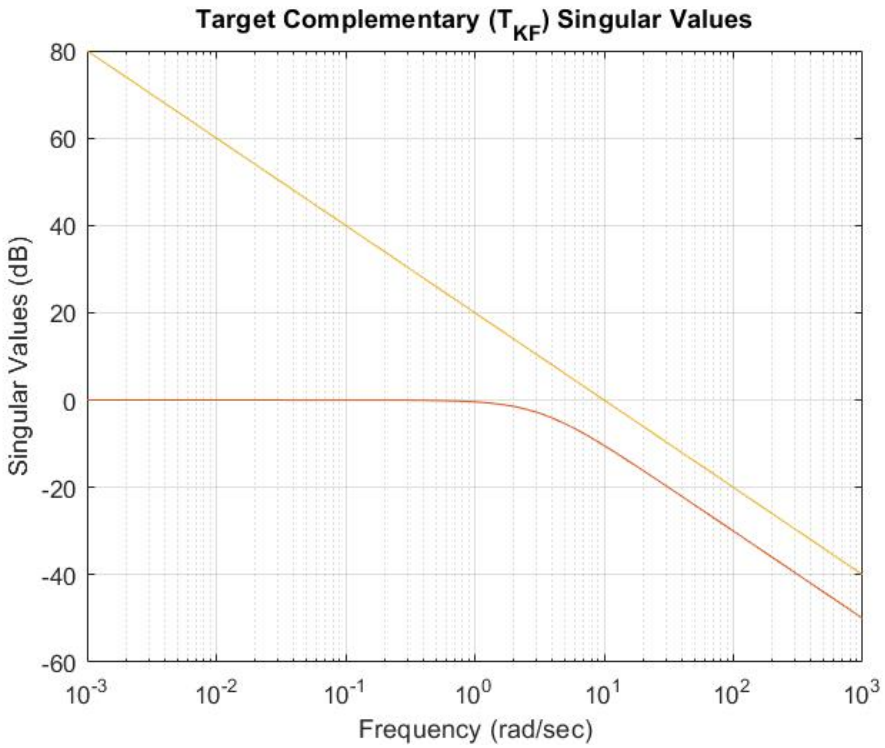

Figure 19: SVD of the Target Complementary Sensitivity using LTR

Open Loop Analysis Breaking the loop at e or y yields the open loop transfer function matrix $\mathbf{L}_e = \mathbf{PK}$. Its singular values are plotted at figure 20. The singular values are matched at low frequencies with a slope of -20dB/dec due to integral action at each input control channel. The plot suggest that low frequency reference command r will be followed, low frequency output disturbance d_o will be attenuated and high frequency noise will be attenuated. Breaking the loop at input u yields the open loop transfer function matrix $L_u = \mathbf{KP}$. It must be emphasized that $\mathbf{KP} \neq \mathbf{PK}$ since matrix multiplication doesnt commute. The associated transfer function matrix is

$$T_{d_i u_p} = \Big[I + \mathbf{KP}\Big]^{-1} = \Big[I + L_u\Big]^{-1} \tag{60}$$

The singular values suggests that input disturbances d_i with frequency content below 0.1 rad/sec will be attenuated by about 20 dB/dec - resulting in a u_p having about one-tenth of the disturbance. Large wiggles in u_p may result in actuator degradation or premature failure. The plot of singular values is shown in figure 21

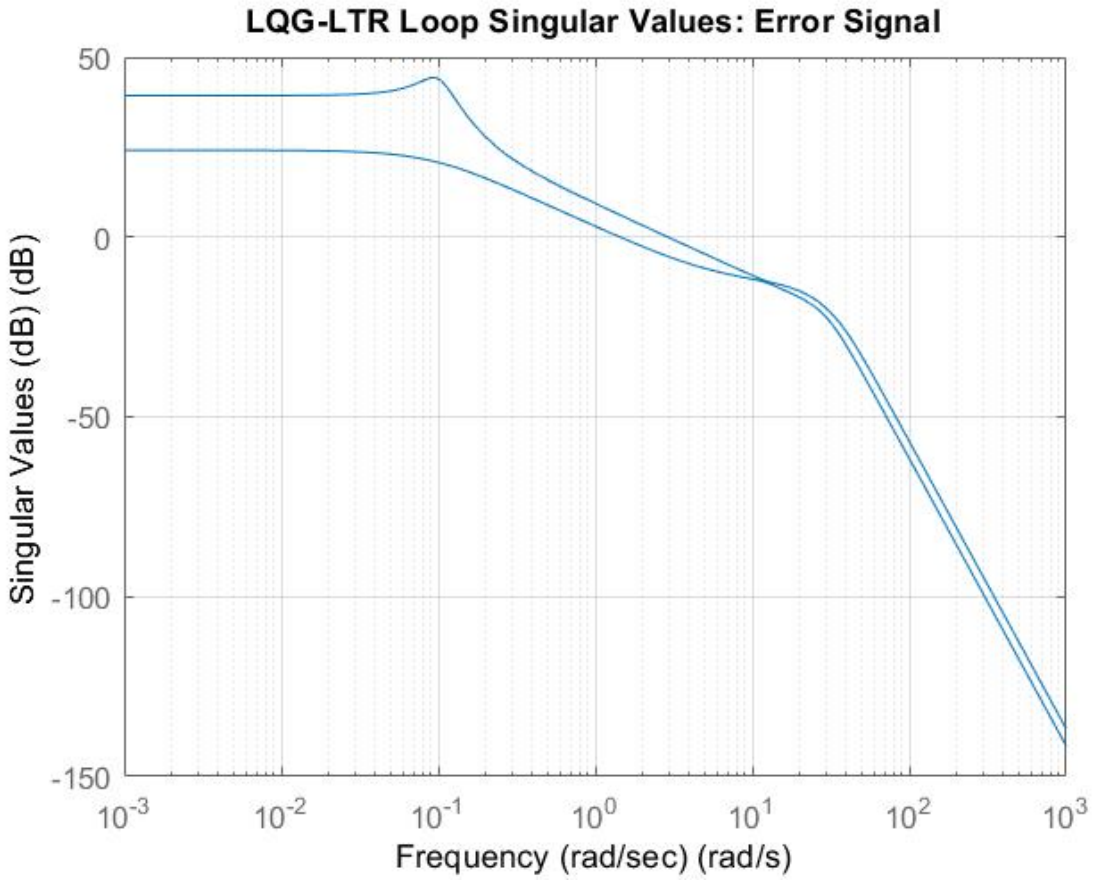

Figure 20: SVD of the Open Loop at error using LTR

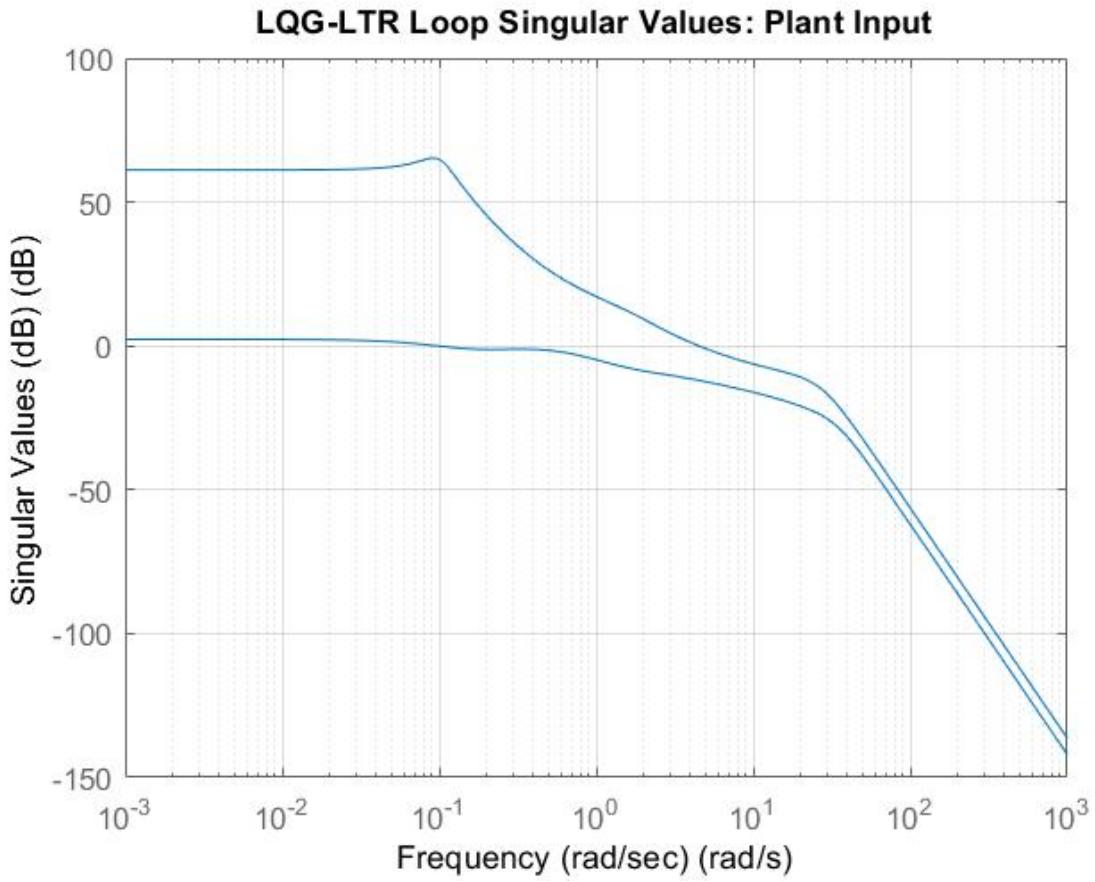

Figure 21: SVD of the Sensitivity at error using LTR

Closed Loop Analysis Sensitivity Frequency Response at error. The sensitivity transfer function matrix associated with e is given by:

$$S_e = \Big[I + \mathbf{PK}\Big]^{-1} = \Big[I + L_e\Big]^{-1} \tag{61}$$

We can see from figure 22 and23 that the values of sensitivity is below -10 dB at low frequencies and that peak values of sensitivity is below 3 dB at input. This ensures that the systems has good robust margins for small gain conditions. Also this signifies that the design has good low frequency command following and good low frequency disturbance attenuation at both input and output of the plant. Since there is RHP-zero present in the system, we cannot indiscriminately push the sensitivity at low frequency as the resulting popping of the sensitivity at higher frequency would not satisfy the bandwidth criteria of the system. The peak of the sensitivity matrix is also important and is associated with near-imaginary axis poles of the resulting closed loop system, which is undesirable. However, the peak sensitivity could not be reduced further for the above mentioned BW consideration. The peak sensitivity is bounded by α. Our design here has a peak sensitivity less that 3.64 dB.

Complementary Sensitivity Frequency Response at Output. The complementary sensitivity frequency response at output or e is given by:

$$T_e = I - S_e = \mathbf{PK}\Big[I + \mathbf{PK}\Big]^{-1} \tag{62}$$

These effective closed loop properties come from the fact that the weighting function for the H_∞ has been chosen according to the ideal conditions for sensitivity and complementary sensitivity. The complementary

sensitivity graph from figure 36 and 35 shows that the system has good high frequency noise attenuation. There is -50 dB noise attenuation after 6.46 rad/sec.The peak sensitivity is bounded by β. Our design here has a peak sensitivity less that 0.205 dB. The K-Sensitivity graph shows how much additive uncertainty can be tolerated by the system. Since our KS is stable, the closed loop system will be stable for all stable additive perturbations Δ_a.

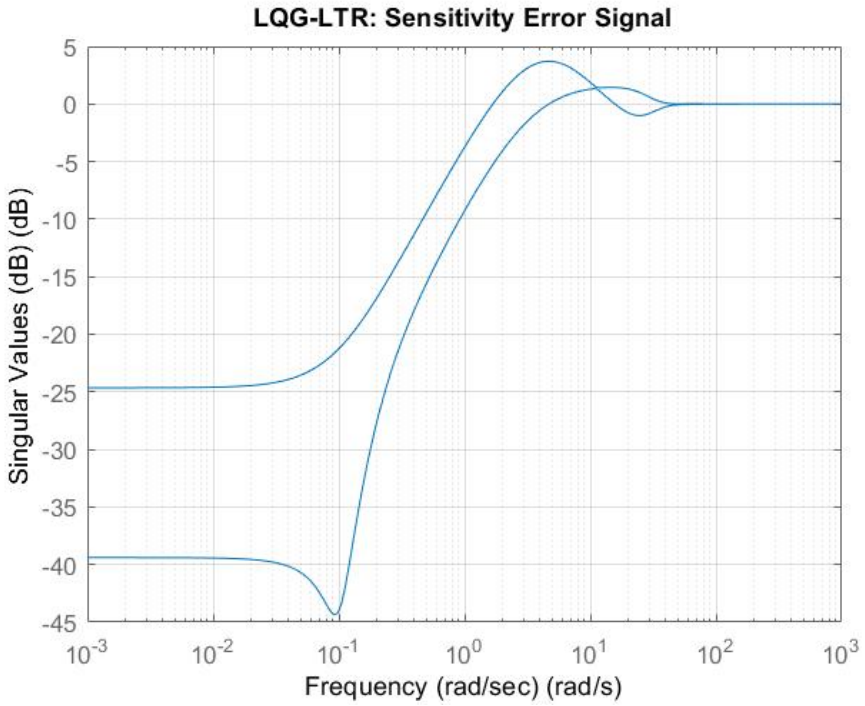

Figure 22: SVD of the Sensitivity at error using LTR

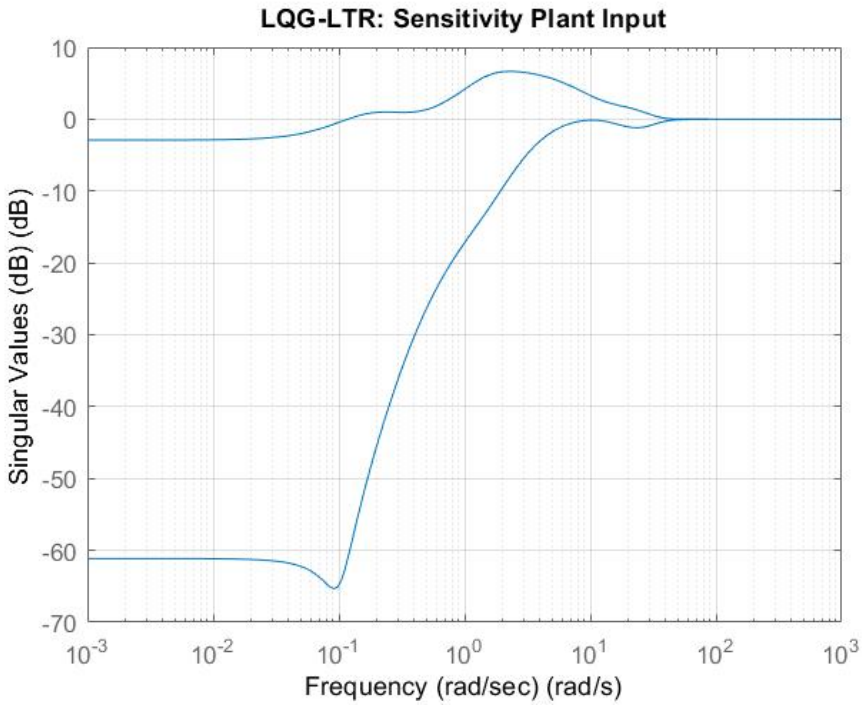

Figure 23: SVD of the Sensitivity at input using LTR

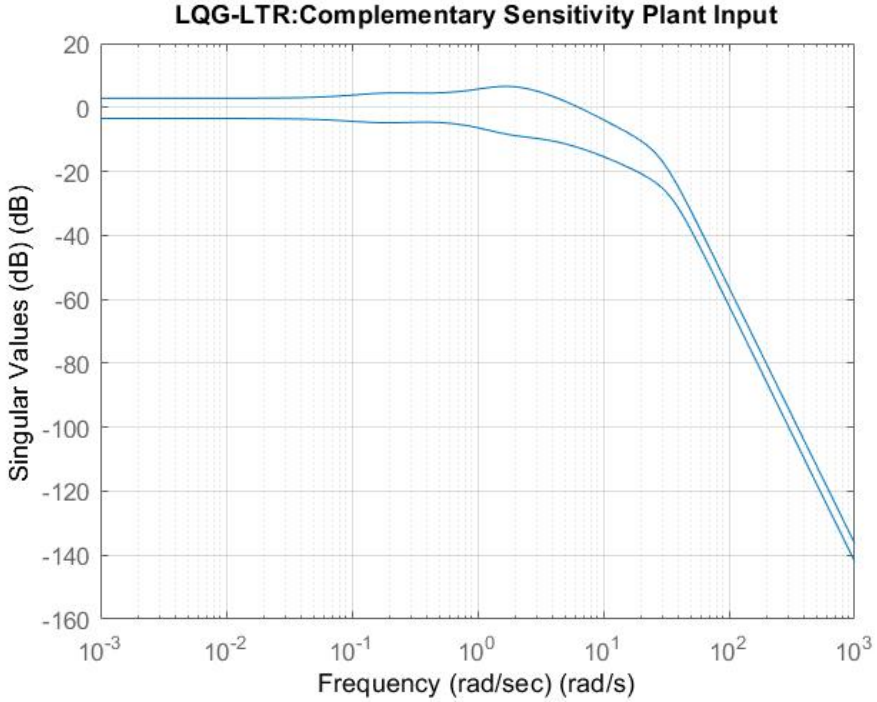

Figure 24: SVD of the Complementary Sensitivity at input using LTR

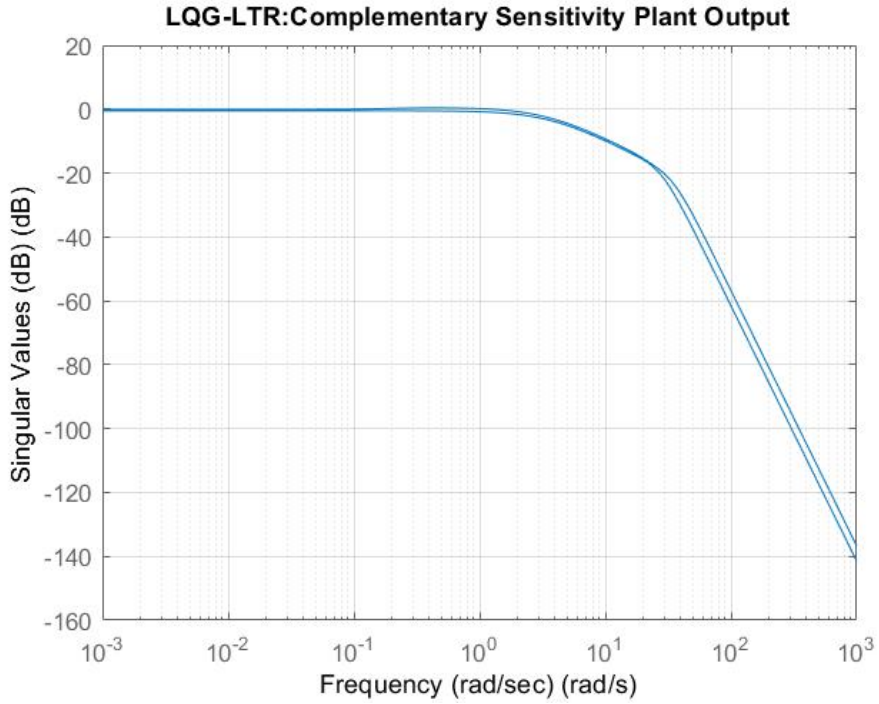

Figure 25: SVD of the Complementary Sensitivity at output using LTR

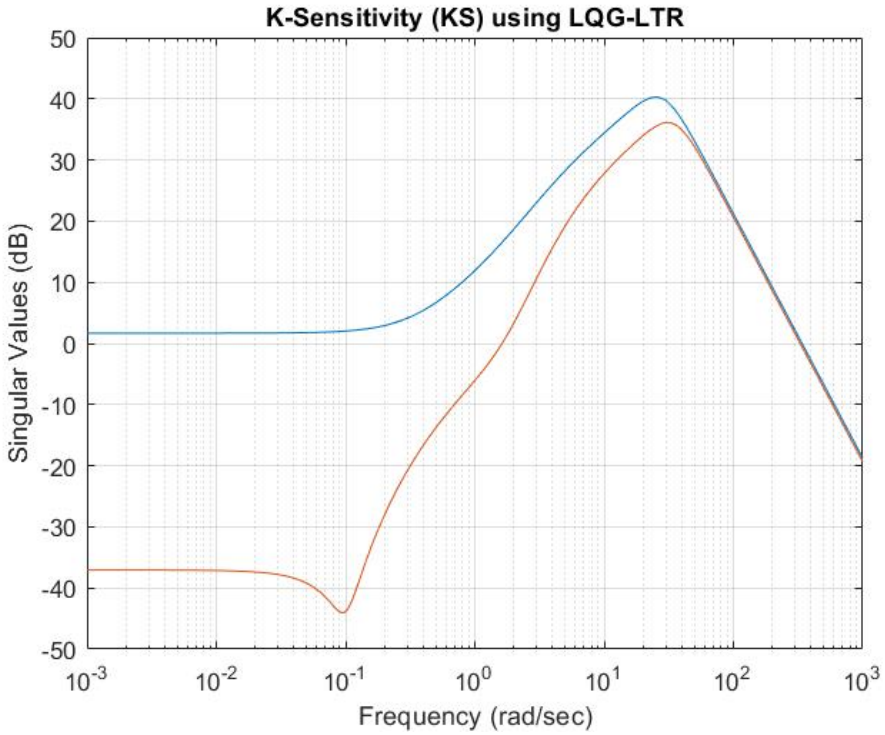

Figure 26: SVD of the K-Sensitivityusing LTR

Time Domain Analysis The Time domain analysis shows that the the system after LQG-LTR design has good command following step responses to both Velocity and FPA. Here the importance is given to reduce overshoot and the settling time is relaxed. In general the overshoot can also be reduced using a pre-filter which will cancel the zeros which gets introduced in the controller. The visualization for the time domain analysis is shown in figure 27.

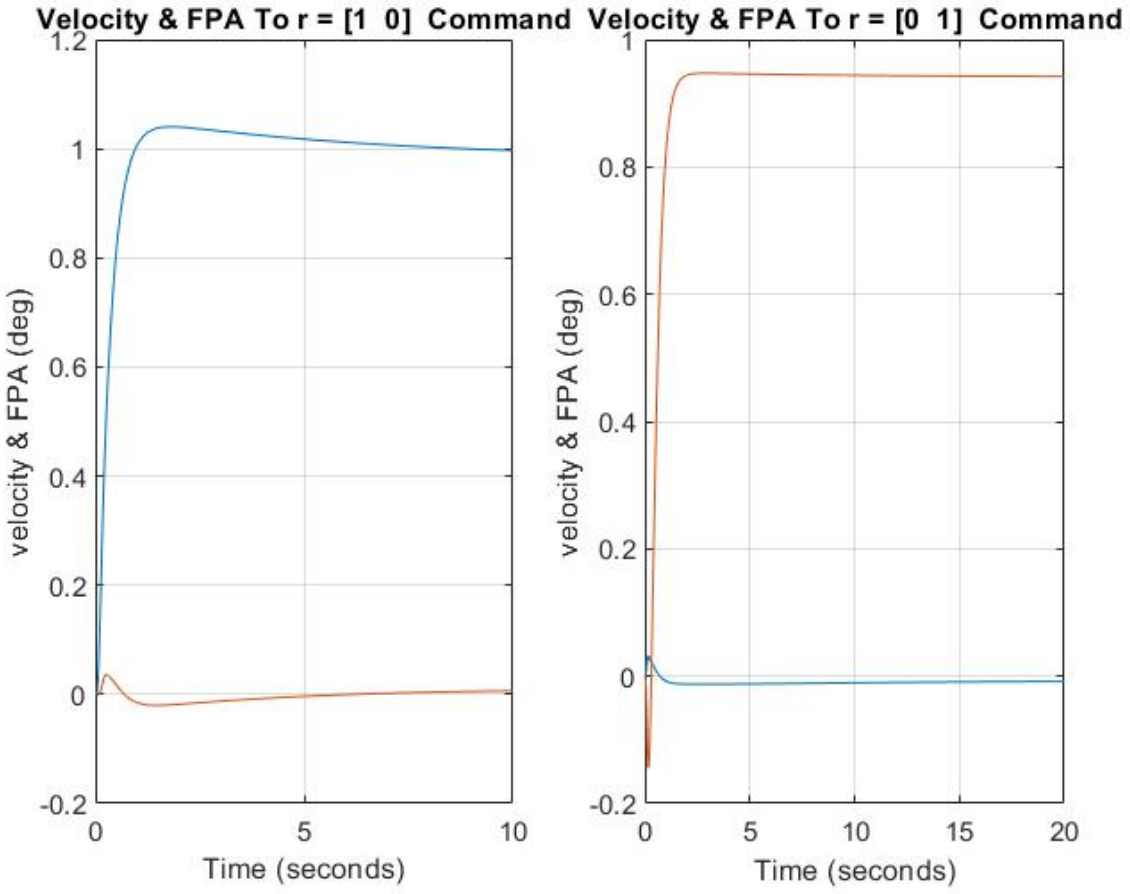

Figure 27: Time domain analysis using LTR

4.5 H_∞ Robust Control Design

Selection of Weighting functions

- *Sensitivity Weighting.* A first order weighting function was selected for W_1.
  1. Initially we started with $\omega_{b1} = \omega_{b2} = 0.01$ rad/sec. This ensures that we are equally aggressive towards FPA steady state errors than velocity steady state errors.
  2. ϵ was chosen to be 0.003 so that we have adequate integral action to make T_doy look small at low frequencies.
  3. As the sensitivity bandwidth parameter ω_{bi} is increased(decreased), the closed loop system bandwidth increases(decreases). For AV-8A Harrier longitudinal dynamics, presence of RHP zero puts an upper bound on the open loop bandwidth. Hence ω_{bi} cannot be arbitrarily increased.
  4. We selected $M_{s1} = M_{s2} = 7$ (16 db) to put an upper bound on the sensitivity peak.
- *Control Sensitivity weighting.* Initially we choose W_2 to be a constant($W_2 = M_u$). This selection did not permit us to roll off KS at higher frequencies to attenuate the sensor noise. It also resulted in larger controls. Hence we select a first order dynamic W_2 as shown previously. This allows us to roll off KS at higher frequencies to ensure attenuation of sensor noise.
  1. (a) We select $\omega_{b1} = \omega_{b2} = 10$ rad/sec. ω_{b1} and ω_{b2} are equal to ensure that we are equally aggressive to throttle action and stick input action.
  2. We select $\epsilon = 0.01$ to roll off the KS singular values at high frequencies to attenuate sensor noise.
  3. We select $M_{ui} = 0.1$ to put an upper bound on the KS peak singular values.
- *Complementary Sensitivity Weighting.* A first order dynamic weighting function was selected for W_3 as shown.
  1. We selected $\omega_{b1} = \omega_{b2} = 20$ rad/sec - one decade above our desired open loop unity gain crossover frequency of 2 rad/sec.
  2. We select $\epsilon = 0.001$ to roll off the singular values at high frequencies to attenuate the sensor noise.
  3. We select $M_{yi} = 2$ (6 db) to put an upper bound on the peaks so that the step responses have minimal overshoot.

Following is the table denoting the the various parameters for the weights W1,W2 and W3:

	W1	W2	W3
M1	7	0.1	2
M2	7	0.1	2
ω_1	0.01	10	20
ω_2	0.01	10	20
ϵ_1	0.003	0.01	0.001
ϵ_2	0.003	0.01	0.001

The weights were obtained by referencing Kaustav Mondal's theseis on fixed wing aircraft [4]. The visualization of the inverse of weighting functions are given in the figure 28,29 and 30.

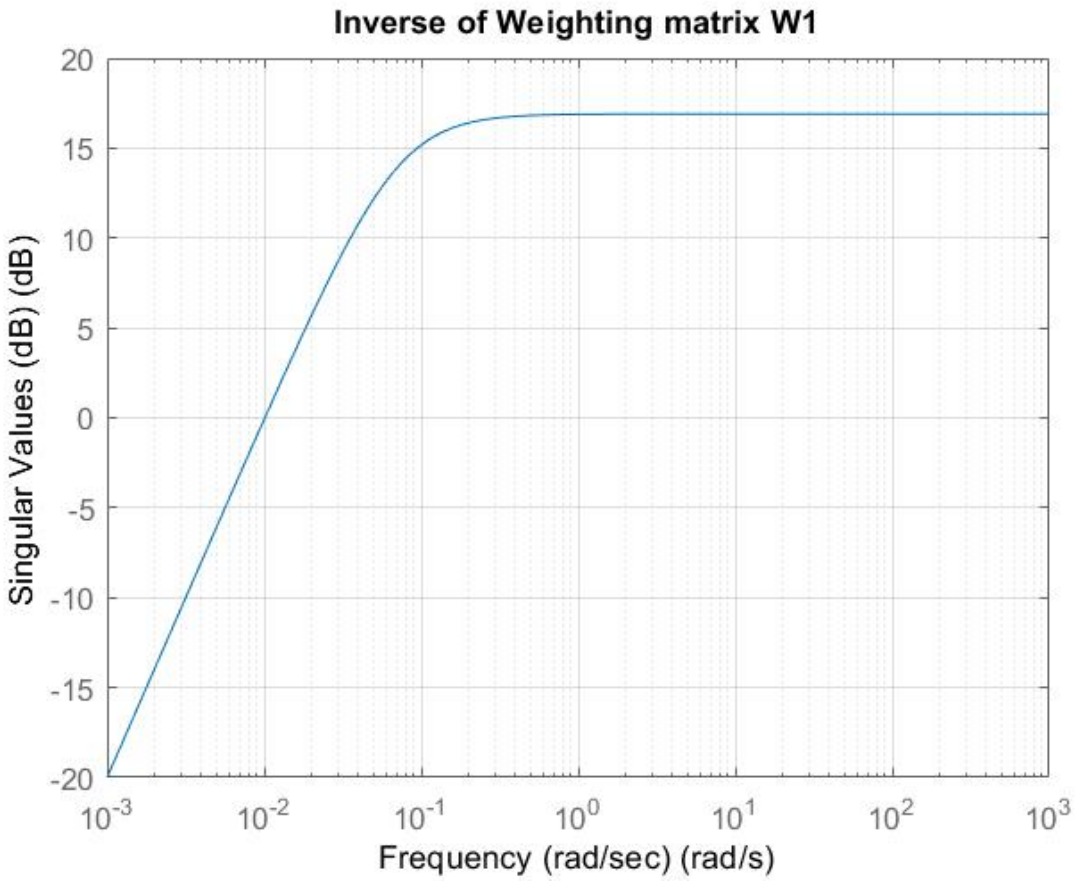

Figure 28: SVD of the Inverse Weighting Function W1

After the selection of weighting functions, the controller was created using *augw* command in MATLAB. Here the bilinear transformation is applied to the nominal plant first and then used in the function along with the W's. Once the generalized plant is obtained, the controller is generated using the *hinfsyn* command of MATLAB. Since Bilinear transformation was first used on the plant, inverse bilinear is used on the generated controller to obtain the final controller. Here we use $p1 = -0.0944$ and $p2 = -10^{20}$.
Poles and Zeros. The zeros and the poles of the controller K is as follows:

	Poles and Zeros of K_{H_∞}
$s_{1,2}$	$-2.0000 \times 1.0e+04$
$s_{3,4}$	$-0.0100 \times 1.0e+04$
s_5	$-0.0012 \times 1.0e+04$
$s_{6,7}$	$-0.0001 \pm 0.0001i \times 1.0e+04$
s_8	$-0.0002 \times 1.0e+04$
$s_{9,10,11,12}$	$-0.0000 \times 1.0e+04$
$z_{1,2}$	$-2.0000 \times 1.0e+04$
$z_{3,4}$	$-0.1000 \times 1.0e+04$
z_5	$-0.0012 \times 1.0e+04$
$z_{6,7}$	0.0000
$z_{8,9}$	$-0.0001 \pm 0.0001i \times 1.0e+04$
z_{10}	-0.0002

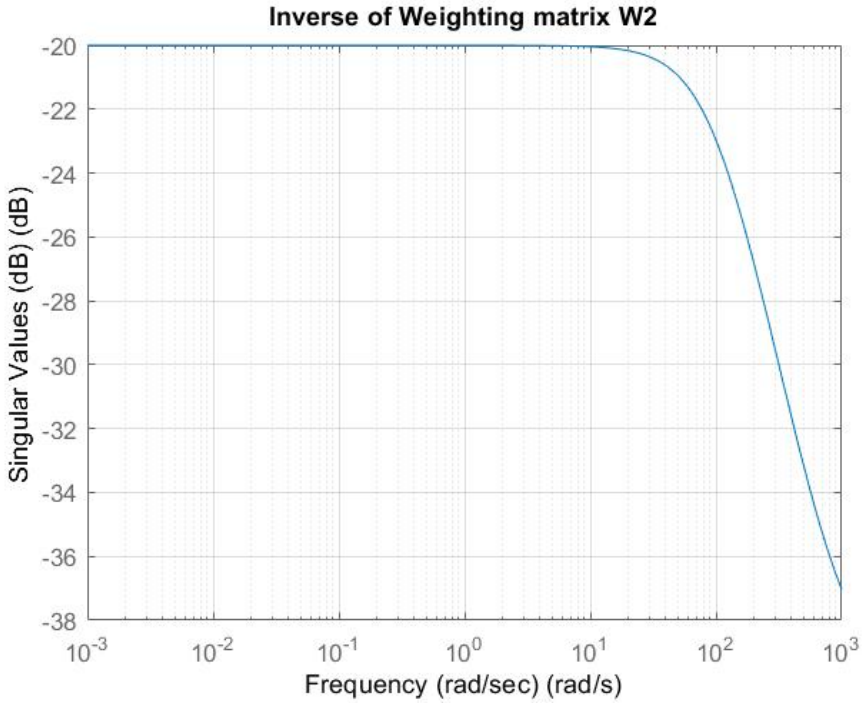

Figure 29: SVD of the Inverse Weighting Function W2

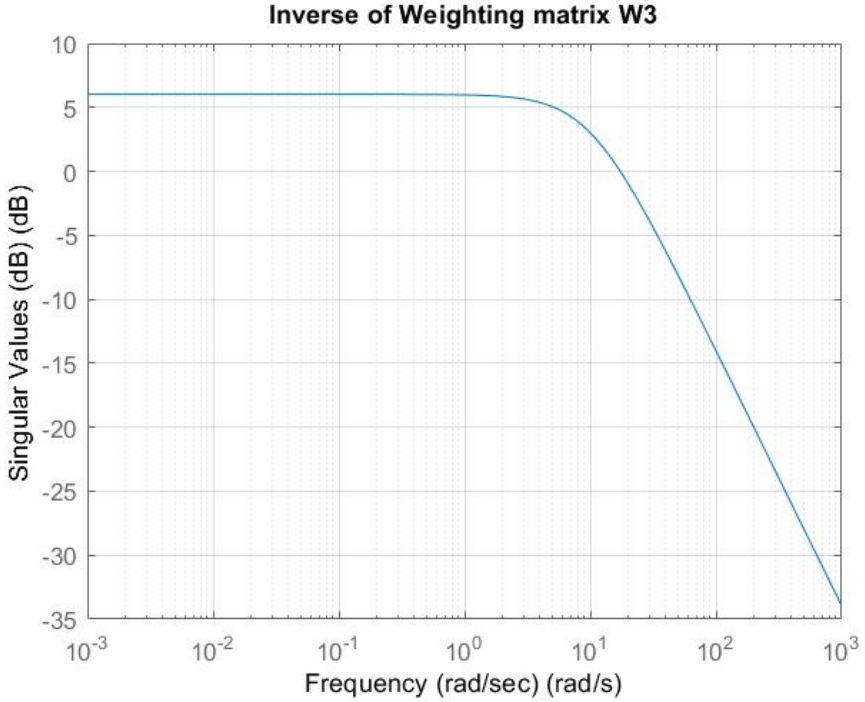

Figure 30: SVD of the Inverse Weighting Function W3

Open loop Analysis. Breaking the loop at e or y yields the open loop transfer function matrix $\mathbf{L}_e = \mathbf{PK}$. Its singular values are plotted at figure 31. The singular values are matched at low frequencies with a slope of -20dB/dec due to integral action at each input control channel. The plot suggest that low frequency reference command r will be followed, low frequency output disturbance d_o will be attenuated and high frequency noise will be attenuated. Breaking the loop at input u yields the open loop transfer function matrix $L_u = \mathbf{KP}$. It must be emphasized that $\mathbf{KP} \neq \mathbf{PK}$ since matrix multiplication doesnt commute. The associated transfer function matrix is

$$T_{d_i u_p} = \Big[I + \mathbf{KP}\Big]^{-1} = \Big[I + L_u\Big]^{-1} \tag{63}$$

The singular values suggests that input disturbances d_i with frequency content below 0.1 rad/sec will be attenuated by about 20 dB/dec - resulting in a u_p having about one-tenth of the disturbance. Large wiggles in u_p may result in actuator degradation or premature failure. The plot of singular values is shown in figure 32.

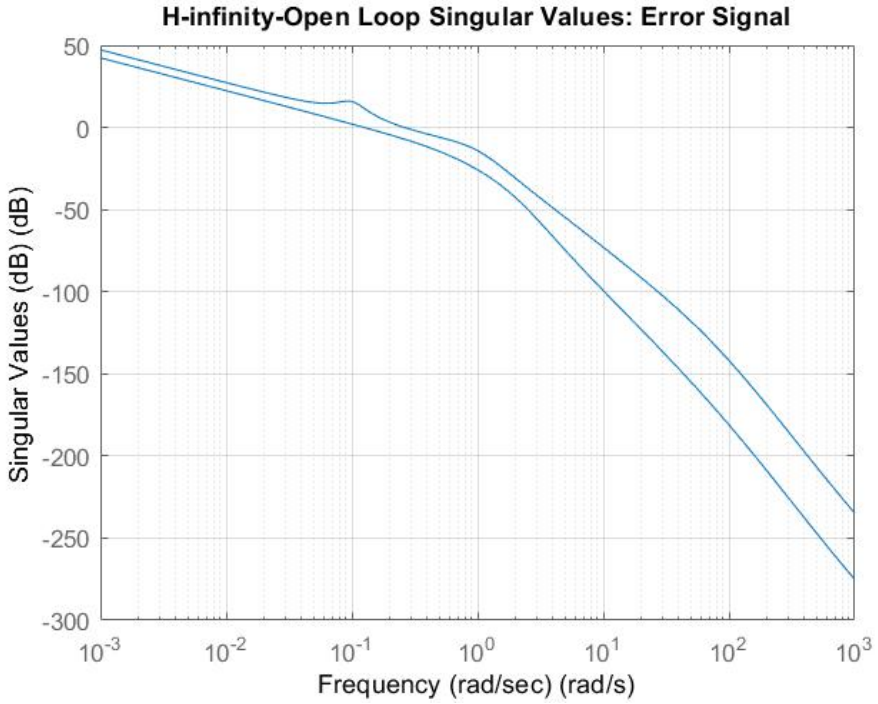

Figure 31: SVD of the H_∞ Open loop error signal

Closed loop Analysis. Poles and zeros of the closed loop systems $\frac{PK}{1+PK}$ is as follows:

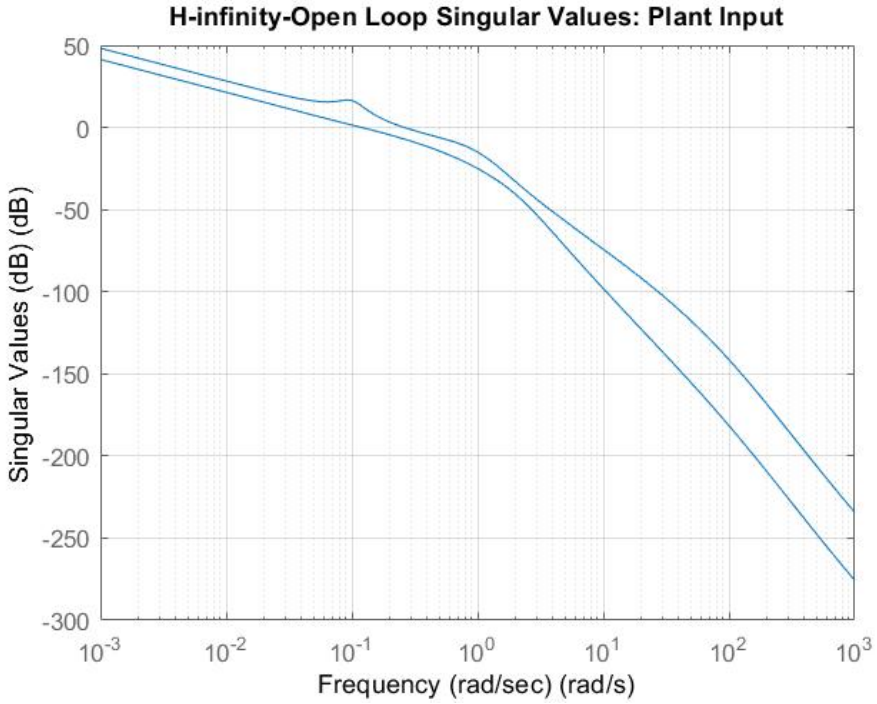

Figure 32: SVD of the H_∞ plant input signal

	Poles and Zeros of PK_{H_∞}
$s_{1,2,3,4}$	$-0.0001 \pm 0.0001i \times 1.0e+04$
$s_{5,6}$	$-0.0002 \times 1.0e+04$
$s_{7,8}$	$-0.0012 \times 1.0e+04$
$s_{9,10}$	$-2.0000 \times 1.0e+04$
$s_{11,12}$	$-0.0100 \times 1.0e+04$
$z_{1,2}$	$-2.0000 \times 1.0e+04$
$z_{3,4}$	$-0.1000 \times 1.0e+04$
z_5	$-0.0012 \times 1.0e+04$
$z_{6,7}$	$0.0006 \times 1.0e+04$
$z_{8,9}$	$0.0007 \times 1.0e+04$
z_{10}	-0.0002

Sensitivity Frequency Response at error. The sensitivity transfer function matrix associated with e is given by:

$$S_e = \Big[I + \mathbf{PK}\Big]^{-1} = \Big[I + L_e\Big]^{-1} \tag{64}$$

We can see from figure 33 and34 that the values of sensitivity is below -10 dB at low frequencies and that peak values of sensitivity is below 2 dB at input. This ensures that the systems has good robust margins for small gain conditions. Also this signifies that the design has good low frequency command following and good low frequency disturbance attenuation at both input and output of the plant. Since there is RHP-zero present in the system, we cannot indiscriminately push the sensitivity at low frequency as the resulting popping of the sensitivity at higher frequency would not satisfy the bandwidth criteria of the system. The peak of the sensitivity matrix is also important and is associated with near-imaginary axis poles of the resulting closed loop system, which is undesirable. The peak sensitivity is bounded by α. Our design here

has a peak sensitivity less that 0.91 dB. This defines the margins of the system.

$$\uparrow GM > 1.18 \tag{65}$$
$$\downarrow GM < 0.867 \tag{66}$$
$$|PM| > 8.79^{\circ} \tag{67}$$
$$\tag{68}$$

Complementary Sensitivity Frequency Response at Output. The complementary sensitivity frequency response at output or e is given by:

$$T_e = I - S_e = \mathbf{PK}\Big[I + \mathbf{PK}\Big]^{-1} \tag{69}$$

These effective closed loop properties come from the fact that the weighting function for the H_∞ has been chosen according to the ideal conditions for sensitivity and complementary sensitivity. The complementary sensitivity graph from figure 36 and 35 shows that the system has good high frequency noise attenuation. There is -50 dB noise attenuation after 0.9 rad/sec. It also provides bounds on the stability robustness margins, the peak complementary sensitivity is bounded by β. β is found to be 4.52 in our system.

$$\uparrow GM > 1.22 \tag{70}$$
$$\downarrow GM < 0.779 \tag{71}$$
$$|PM| > 12.70^{\circ} \tag{72}$$
$$\tag{73}$$

There is a significant tradeoff between achieving the desired settling time and appropriate margins for the system. The presence of RHP-zero places a huge constraint on how much bandwidth one can achieve to get good **S**,**T** and **KS**. One can achieve better loop shaping with further improvement and tuning of the selection weights. The K-Sensitivity graph shows how much additive uncertainty can be tolerated by the system. Since our KS is stable, the closed loop system will be stable for all stable additive perturbations Δ_a.

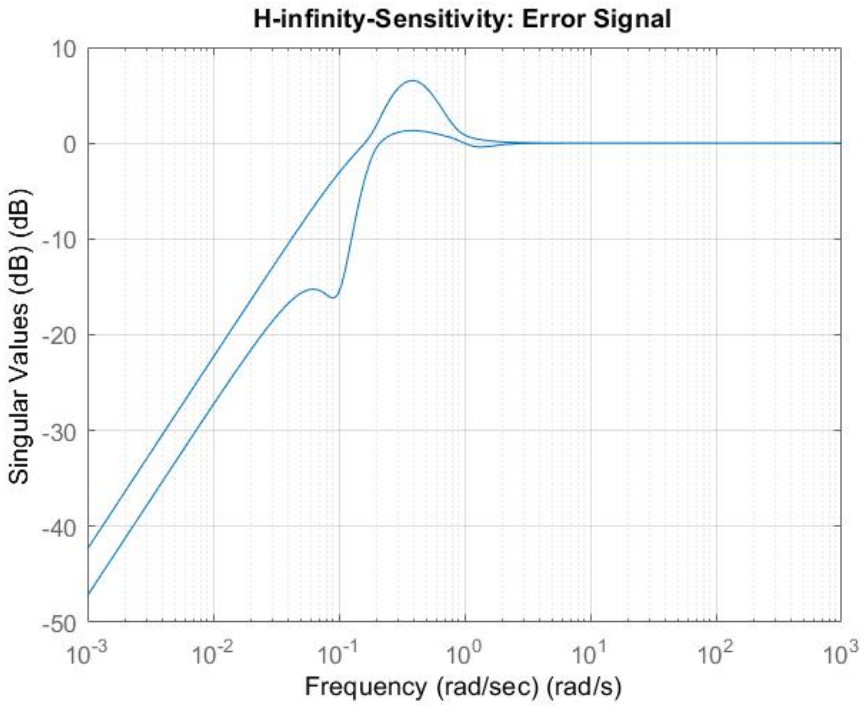

Figure 33: SVD of the H_∞ Sensitivity: error signal

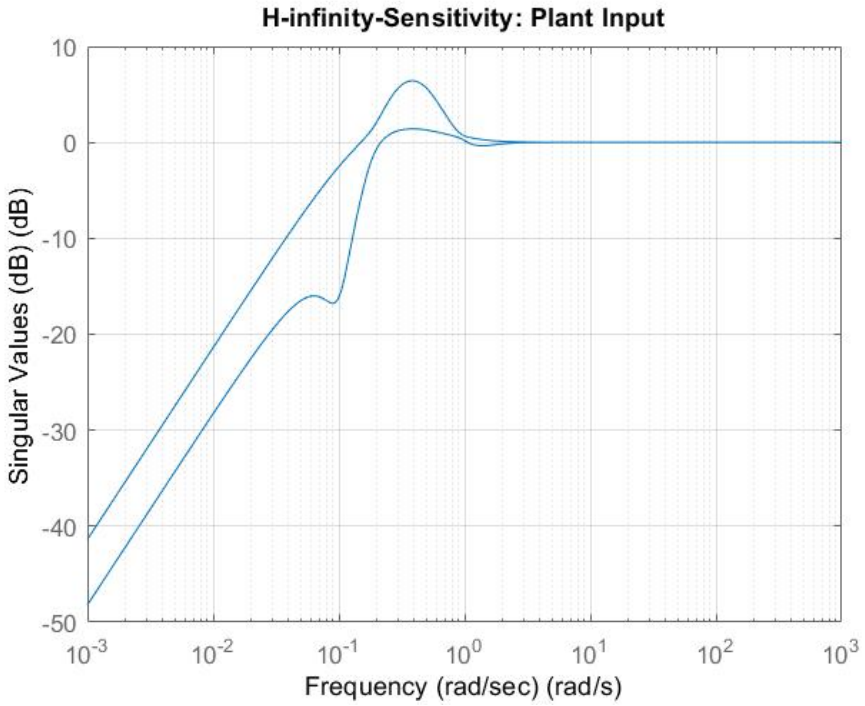

Figure 34: SVD of the H_∞ Sensitivity Input signal

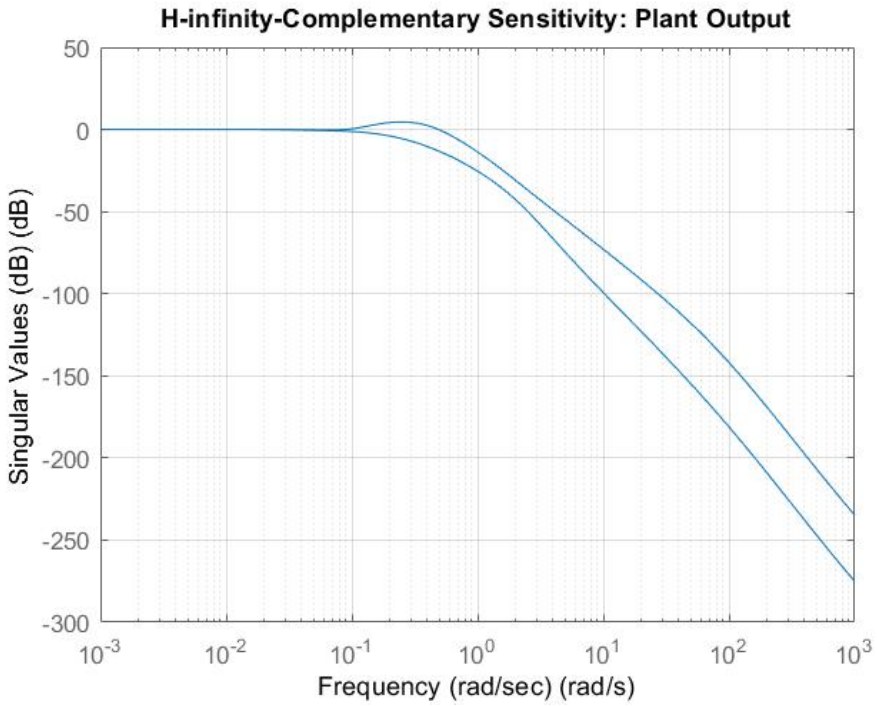

Figure 35: SVD of the H_∞ Complementary Sensitivity Output signal

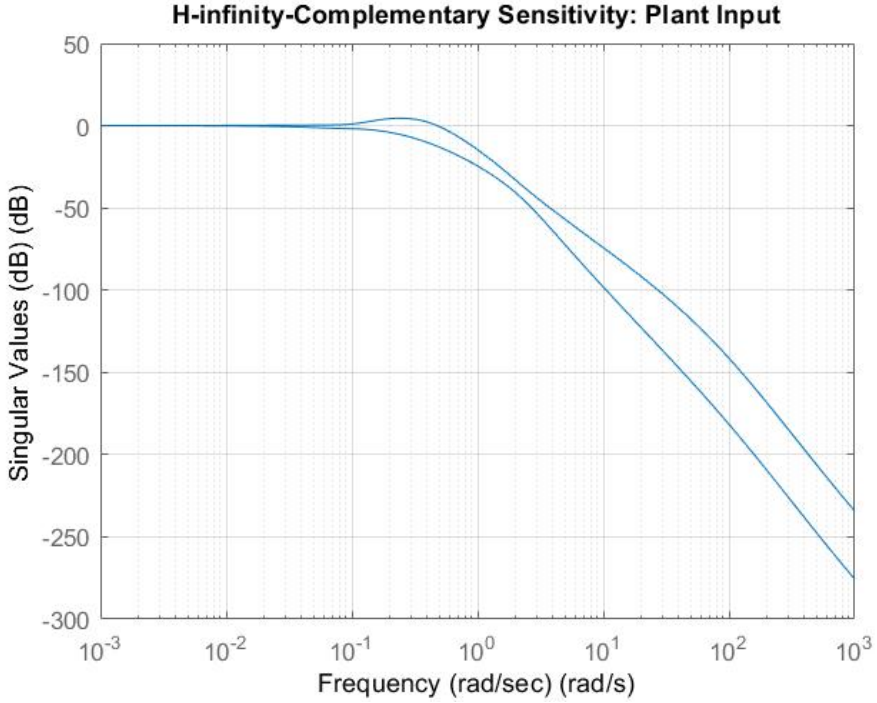

Figure 36: SVD of the H_∞ Complementary Sensitivity Input signal

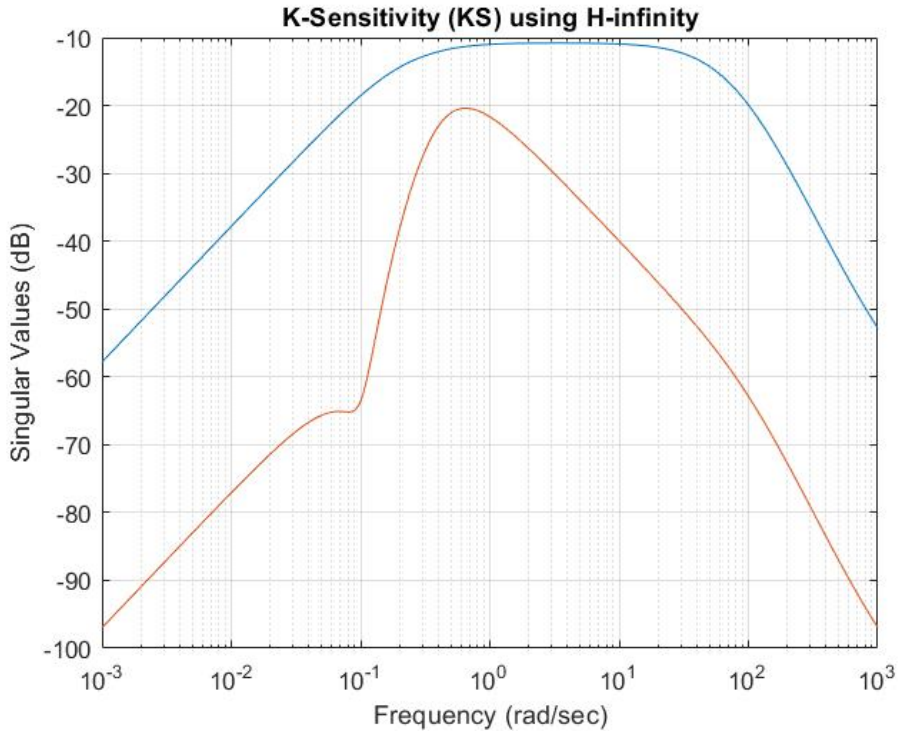

Figure 37: SVD of the H_∞ K-Sensitivity

Time Domain Analysis The Time domain analysis shows that the the system after H_∞ design has good command following step responses to both Velocity and FPA. Here the importance is given to reduce overshoot and the settling time is relaxed. In general the overshoot can also be reduced using a pre-filter which will cancel the zeros which gets introduced in the controller. The visualization for the time domain analysis is shown in figure 38.

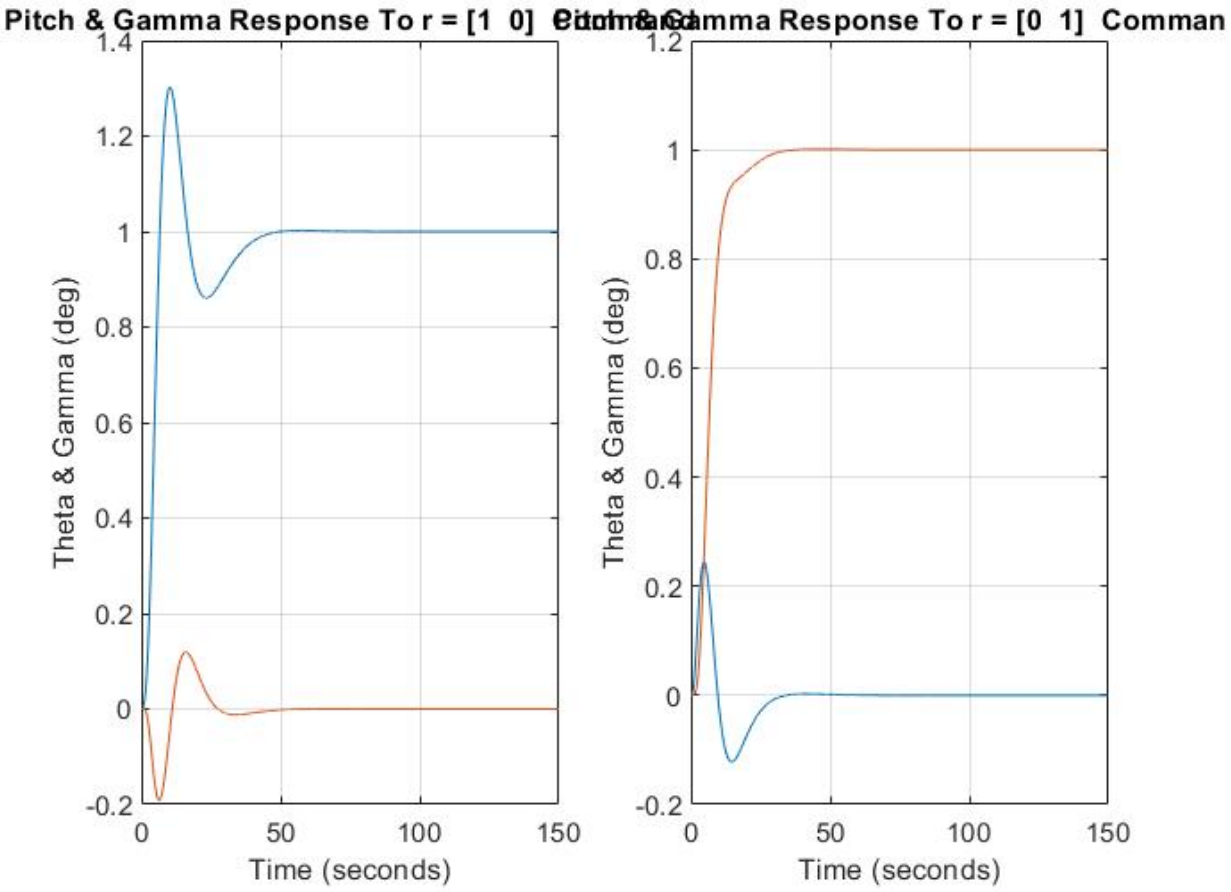

Figure 38: Time domain analysis using H_∞

References

[1] Armando A. Rodriguez, *Modelling of MIMO Dynamical Systems* [*Linear Systems, Analysis and Design, Appendix C*]: 779-780.

[2] Skogestad, Sigurd and Postlethwaite, Ian *Multivariable Feedback Control: Analysis and Design* [John Wiley and Sons, Inc.,USA]:Page(186-235)

[3] Wikipedia contributors. (2018, September 28). Aircraft dynamic modes. In Wikipedia, The Free Encyclopedia. Retrieved 05:13, May 2, 2019, from `https://en.wikipedia.org/w/index.php?title=Aircraft_dynamic_modes&oldid=86160622`

[4] Kaustav Mondal *Multivariable Control of Fixed Wing Aircrafts*Master's thesis at Arizona State University.

5 APPENDIX-I

MATLAB CODE for AV8A Harrier longitudinal dynamics To run the code one must have the `Harrier.m` file and `f_CLFTM.m` function file in the same directory. Adding the main `Harrier.m` file along with this document.

```
%% EEE588/ Design of Multi variable feedback control system
%Final Project of EEE588
%Topic: AV8A Harrier Aircraft Longitudinal Dynamicss
%Modelling of plant which includes Actuator and Engine dynamics
%of the motors.
%*************************************************************************
%Model of the plant
%Ap, Bp, Cp, Dp
%After including actuator there are total 6 states and 2 inputs and 2
%outputs.
%
clear all;
clc;
close all;
Ap= [0 1 0 0 0 0;
     1.837  1.893 1.837  0.0004 0.0062  0.1243;
    0.5295 0.0085  0.5295 0.0006 0.0002 0.0017;
     34.5 0 2.3  0.0621 0.4209  0.0452;
    0 0 0 0  1.966 0;
    0 0 0 0 0  12];
Bp= [0 0;
    0 0;
    0 0;
    0 0;
    1.966 0;
    0 12;];
Cp= [0 0 0 1 0 0;
    0 0 57.2958 0 0 0];
Dp= 0*ones(2,2);

P = ss(Ap,Bp,Cp,Dp); %Nominal Plant model
%*************************************************************************
%% Plant Dimensions
%
[ns,nc] = size(Bp);                    % Number of States, Number of Controls
no      = nc;                          % Number of Outputs
%% Modal Analysis   Eigenvalue EigenVector function
%Natural Modes:

[evec,eval] = eig(Ap); %Poles of nominal plant

%*************************************************************************
%% Transmission Zeros
%
plantzeros = tzero(ss(Ap,Bp,Cp,Dp))        % transmission zeros
%zdir = null([z*eye(4) Ap  Ap; Cp Dp])    % transmission zero directions
%*************************************************************************
%% SYSTEM TRANSFER FUNCTIONS: From u_i to y_j
```

```
%
Plant_zpk = zpk(ss(Ap,Bp,Cp,Dp)) % Zeros, Poles, and Gains from u_i to x_j

%% Controllability and Observability
%
% Controllability
%
CM  = [Bp Ap*Bp (Ap^2)*Bp  (Ap^3)*Bp];%   (ap^4)*bp ]  % Controllability Matrix
rcm = rank(CM)                                        % Rank of Controllability Matrix
%
% system is controllable; that is, rank of controllability matrix is 6
%
%%%%%%%%%%%%%%%%%%%%%%%%%%%%%%%%%%%%%%%%%%%%%%%%%%%%%%%%%%%%%%%%%%%%%%%%%%%
%
% Observability
%
OM  = [Cp;Cp*Ap; Cp*(Ap^2);Cp*(Ap^3)]; %Cp*(ap^4) ]          % Observability Matrix
rom = rank(OM)                 % Rank of Observability Matrix
%
% system is observable; that is, rank of observability matrix is 6
%
%%%%%%%%%%%%%%%%%%%%%%%%%%%%%%%%%%%%%%%%%%%%%%%%%%%%%%%%%%%%%%%%%%%%%%%%%%%
%% Modal analysis
% Visualization of Phugoid Mode (Alpha approximately Constant)
%
% this lightly damped mode takes very long to decay
% the aircraft climbs and drops exchanging kinetic and potential energy
%
t1 = [0:0.05:500];
x = lsim(ss(Ap,Bp, eye(6,6), 0*ones(6,2)), [0*t1; 0*t1] ,t1, real(evec(:,3)) );
figure,
subplot(1,2,1)
plot(t1,x)
grid
title('Visualization of F8 Phugoid Mode (x_o = Re x_{ph})')
xlabel('time (seconds)')
ylabel('x(t)')
%
x = lsim(ss(Ap,Bp, eye(6,6), 0*ones(6,2)), [0*t1; 0*t1] , t1, imag(evec(:,3)) );
subplot(1,2,2)
plot(t1,x)
grid
title('Visualization of F8 Phugoid Mode (x_o = Imag x_{ph})')
xlabel('time (seconds)')
ylabel('x(t)')
%
% Visualization of Short Period Mode (Speed approximately Constant)
%
% this lightly damped mode decays very quickly
%
t1 = [0:0.05:5];
x = lsim(ss(Ap,Bp, eye(6,6), 0*ones(6,2)), [0*t1; 0*t1] , t1, real(evec(:,1)) );
figure,
subplot(1,2,1)
```

```
plot(t1,x)
grid
title('Visualization of F8 Short Period Mode (x_o = Re x_{sp})')
xlabel('time (seconds)')
ylabel('x(t)')
%
x = lsim(ss(Ap,Bp, eye(6,6), 0*ones(6,2)), [0*t1; 0*t1] , t1, imag(evec(:,1)) );
subplot(1,2,2)
plot(t1,x)
grid
title('Visualization of F8 Short Period Mode (x_o = Im x_{sp})')
xlabel('time (seconds)')
ylabel('x(t)')
%% Frequency Response: Singular Values of Plant
P = ss(Ap,Bp,Cp,Dp);
winit  =  3;
wfin   =  3;
nwpts  = 200;
w      = logspace(winit,wfin,nwpts);    % Form vector of logarithmically spaced freq points
sv_p     = sigma(P,w);
sv_p     = 20*log10(sv_p);
figure; semilogx(w, sv_p)
%clear sv
title('SVD of nominal plant')
grid
xlabel('Frequency (rad/sec)')
ylabel('Singular Values (dB)')

%%%%%%%%%%%%%%%%%%%%%%%%%%%%%%%%%%%%%%%%%%%%%%%%%%%%%%%%%%%%%%%%%%%%%%%%%%%%%%%
%
% SVD ANALYSIS at DC
%
dc =  Cp*inv( Ap)*Bp + Dp;
[udc,sdc,vdc] = svd(dc);

G_o = udc*sdc*vdc;


figure,
subplot(2,2,1)
bar(sdc(1,1)*udc(1,:))
title('\sigma_11*u1')
grid
xlabel('Output [vel FPA]')
ylabel('\sigma_11*u1')
subplot(2,2,2)
bar(vdc(:,1))
title('v1')
grid
xlabel('Controls [stick_input throttle ]')
ylabel('v1')
%%%%%%%%%%%%%%%%%%%%%%%%%%%%%%%%%%%%%%%%%%%%%%%%%%%%%%%%%%%%%%%%%%%%%%%%%%%%%%%
subplot(2,2,3)
bar(abs(sdc(2,2)*udc(2,:)))
```

```
title('\sigma_22*u2')
grid
xlabel('Output [vel FPA]')
ylabel('\sigma_22*u2')
subplot(2,2,4)
bar(abs(vdc(:,2)))
title('v2')
grid
xlabel('Controls [stick_input throttle]')
ylabel('v2')


%************************************************************************
%
% SVD Analysis at a selected frequency
%
s1 = j*0.0975;                                          % At Phugoid Mode
g1 = Cp*inv(s1*eye(6) Ap)*Bp + Dp;
[u1, sing1, v1 ] = svd(g1);
v1mag = abs(v1);
v1phase = angle(v1)*180/pi;
u1mag = abs(u1);
u1phase = angle(u1)*180/pi;

%************************************************************************
%
% SVD Analysis at a selected frequency
%
s2 = j*1.1672;                                          % At Short Period Mode
g2 = Cp*inv(s2*eye(6) Ap)*Bp + Dp;
[u2, sing2, v2 ] = svd(g2);
v2mag = abs(v2);
v2phase = angle(v2)*180/pi;
u2mag = abs(u2);
u2phase = angle(u2)*180/pi;


%************************************************************************
%% Augment Plant with Integrators at Plant Input and Plot Singular Values
Ad=[Ap Bp
    0*ones(nc,ns) 0*ones(nc,nc)];
Bd=[0*ones(ns,nc)
     eye(nc)];
Cd=[Cp 0*ones(nc,nc)];
Dd=0*ones(nc,nc);

%************************************************************************
% Plant analysis after augmentation
Pd=ss(Ad,Bd,Cd,Dd);
pp=eig(Pd);% Eigen values of new plant
ptz=tzero(Pd);%transmission zeros of new plant

figure;
sv_aug=sigma(Pd,w);
```

```
tsv_aug=20*log10(sv_aug);
semilogx(w,tsv_aug);
title('SVD of the plant after Dynamic Augmentation');
grid on;
xlabel('Frequency (rad/sec)');
ylabel('Singular Values (dB)');



%%%%%%%%%%%%%%%%%%%%%%%%%%%%%%%%%%%%%%%%%%%%%%%%%%%%%%%%%%%%%%%%%%%%%%%%%%%%%%%
%% Bilinear transformation
p1= 0.0944; p2= 1e20;
[A_blin,B_blin,C_blin,D_blin]=bilin(Ad,Bd,Cd,Dd,1,'Sft_jw',[p2 p1]);
%%%%%%%%%%%%%%%%%%%%%%%%%%%%%%%%%%%%%%%%%%%%%%%%%%%%%%%%%%%%%%%%%%%%%%%%%%%%%%%
% Plant analysis after Bilinear
Pd_lin=ss(A_blin,B_blin,C_blin,D_blin);
[evec_alin,eval_alin] = eig(A_blin);%eigenvalues after bilinear trans
auglin_plantzeros = tzero(ss(A_blin,B_blin,C_blin,D_blin));%transmission zeros after biline
figure;
sv_lin=sigma(Pd_lin,w);
tsv_lin=20*log10(sv_lin);
semilogx(w,tsv_lin);
title('SVD of the plant after Bilinear transformation');
grid on;
xlabel('Frequency (rad/sec)');
ylabel('Singular Values (dB)');
%%%%%%%%%%%%%%%%%%%%%%%%%%%%%%%%%%%%%%%%%%%%%%%%%%%%%%%%%%%%%%%%%%%%%%%%%%%%%%%
%% LQR Design

Q=C_blin'*C_blin;
rho = 1e12;
R = rho*eye(nc);
%
% [G, poles, K] = lqr(A_blin,B_blin,Q,R);
% Q = eye(8)% State Weighting Matrix
% % Q1(1,1) = 2000;
% % Q1(2,2) = 100;
%  Q(3,3) = 10;
%  Q(4,4) = 1;
% rho = 1e9;                                          % Cheap control recovery parameter
                                                    % The smaller the parameter, the bette
R = rho*eye(nc)                                     % Control Weigthing Matrix
[G, K, poles] = lqr(A_blin,B_blin,Q,R);
Glqr=ss(A_blin,B_blin,G,0);
lqrp=eig(A_blin,B_blin*G);
lqrtz=tzero(Glqr);

[Ak,Bk,Ck,Dk]=bilin(Glqr.A,Glqr.B,Glqr.C,Glqr.D, 1,'Sft_jw',[p2 p1]);
K1=ss(Ak,Bk,Ck,Dk);

So1=inv(eye(size(K1))+K1);
To1=eye(size(K1)) So1;

figure;
```

```
sv=sigma(So1,w);
tsv=20*log10(sv);
semilogx(w,tsv);
title('Sensitivity (S) using LQR');
grid on;
xlabel('Frequency (rad/sec)');
ylabel('Singular Values (dB)');

figure;
sv=sigma(To1,w);
tsv=20*log10(sv);
semilogx(w,tsv);
title('Complementary Sensitivity (T) using LQR');
grid on;
xlabel('Frequency (rad/sec)');
ylabel('Singular Values (dB)');

% t = [0:0.02:5];
% [y, t, x] = step(To1,t);
% figure;
% plot(t,y(:,:,2))
% grid
% title('Pitch & Gamma Response To r = [1   0]  Command')
% ylabel('Theta & Gamma (deg)')
% xlabel('Time (seconds)')
%%%%%%%%%%%%%%%%%%%%%%%%%%%%%%%%%%%%%%%%%%%%%%%%%%%%%%%%%%%%%%%%%%%%%%%%%%%
%% Kalman filter
Pint=eye(nc);
mu=0.1;
Mint=mu*eye(nc);
[Kkf, H, sig]=kalman(Pd_lin,Pint,Mint);
Gkf=ss(A_blin H*C_blin,H, C_blin,0);

% Plant analysis after Kalman filter
kfp=eig(A_blin H*C_blin);
kftz=tzero(Gkf);
%%%%%%%%%%%%%%%%%%%%%%%%%%%%%%%%%%%%%%%%%%%%%%%%%%%%%%%%%%%%%%%%%%%%%%%%%%%
%% LQG Design
%
% Am=A_blin  B_blin*G H*C_blin;
% Bm=H;
% Cm=G;
% Dm=0;
% Glqg=ss(Am,Bm,Cm,Dm);

%Form final compensator
Am = [0*ones(2,2)  G;
      0*ones(8,2) A_blin  B_blin*G H*C_blin];
Bm = [0*ones(2,2);
       H];
Cm = [eye(2,2) 0*ones(2,8)]

Dm = [0*ones(2,2)];
Glqg =ss(Am,Bm,Cm,Dm);
```

```
%%%%%%%%%%%%%%%%%%%%%%%%%%%%%%%%%%%%%%%%%%%%%%%%%%%%%%%%%%%%%%%%%%%%%%%%%%%%
% Analysis after LQG augmentation

lqgp=eig(A_blin  B_blin*G H*C_blin);
lqgtz=tzero(Glqg);

[Ak,Bk,Ck,Dk]=bilin(Glqg.A,Glqg.B,Glqg.C,Glqg.D, 1 ,'Sft_jw',[p2  p1]);
K2=ss(Ak,Bk,Ck,Dk);
[Lo2,Li2,So2,Si2,To2,Ti2,KS2,SP2]=f_CLTFM(P,K2);

%%%%%%%%%%%%%%%%%%%%%%%%%%%%%%%%%%%%%%%%%%%%%%%%%%%%%%%%%%%%%%%%%%%%%%%%%%%%
%
% OPEN LOOP FREQUENCY RESPONSE
figure;
sigma(Lo2,w);
title('LQG Loop Singular Values: Error Signal')
grid
xlabel('Frequency (rad/sec)')
ylabel('Singular Values (dB)')

figure;
sigma(Li2,w);
title('LQG Loop Singular Values: Plant Input')
grid
xlabel('Frequency (rad/sec)')
ylabel('Singular Values (dB)')

%%%%%%%%%%%%%%%%%%%%%%%%%%%%%%%%%%%%%%%%%%%%%%%%%%%%%%%%%%%%%%%%%%%%%%%%%%%%
%
% CLOSED LOOP FREQUENCY RESPONSE

figure;
sigma(So2,w);
title('LQG: Sensitivity Error Signal')
grid
xlabel('Frequency (rad/sec)')
ylabel('Singular Values (dB)')

figure;
sigma(Si2,w);
title('LQG: Sensitivity Plant Input')
grid
xlabel('Frequency (rad/sec)')
ylabel('Singular Values (dB)')

figure;
sigma(To2,w);
title('LQG: Complementary Sensitivity Plant Output')
grid
xlabel('Frequency (rad/sec)')
ylabel('Singular Values (dB)')

figure;
sigma(Ti2,w);
```

```
title('LQG: Complementary Sensitivity Plant Input')
grid
xlabel('Frequency (rad/sec)')
ylabel('Singular Values (dB)')

figure;
sv=sigma(KS2,w);
tsv=20*log10(sv);
semilogx(w,tsv);
title('K Sensitivity (KS) using LQG');
grid on;
xlabel('Frequency (rad/sec)');
ylabel('Singular Values (dB)');
%****************************************************************************
% Time response
t = [0:0.02:10];
[y, t, x] = step(To2,t);
figure;
subplot(1,2,1)
plot(t,y(:,:,1))
grid
title('Velocity & FPA To r = [1  0]  Command')
ylabel('velocity & FPA (deg)')
xlabel('Time (seconds)')

t = [0:0.02:20];
[y, t, x] = step(To2,t);
subplot(1,2,2)
plot(t,y(:,:,2))
grid
title('Velocity & FPA To r = [0  1]  Command')
ylabel('velocity & FPA (deg)')
xlabel('Time (seconds)')
%****************************************************************************
%% LQG LTR Design
%
% Design of Target Loop Singular Values Using Kalman Filter
%
ll =  inv(Cp*inv( Ap)*Bp + Dp);
lh =  inv(Ap)*Bp*ll;
l = [lh;ll];

figure;
sv = sigma(ss(A_blin, l, C_blin, D_blin),w);
sv = 20*log10(sv);
semilogx(w, sv)
title('Filter Open Loop (G_FOL)')
grid
xlabel('Frequency (rad/sec)')
ylabel('Singular Values (dB)')
%****************************************************************************
Pint=eye(nc);
mu=0.1;
Mint=mu*eye(nc);
```

```
[Kkf1, H1, sig]=kalman(ss(A_blin, [B_blin 1], C_blin, [D_blin 0*ones(nc,nc)]),Pint,Mint);

% Recover Target Loop By Solving Cheap LQR Problem
%
Q1 = C_blin'*C_blin;
% Q1 = eye(8)% State Weighting Matrix
% % Q1(1,1) = 2000;
% % Q1(2,2) = 100;
%  Q1(3,3) = 10;
%  Q1(4,4) = 100;
rho = 1e 9;                                          % Cheap control recovery parameter;
                                                     % The smaller the parameter, the bette
R1 = rho*eye(nc)                                     % Control Weigthing Matrix
[G1, poles, rrr] = lqr(A_blin,B_blin,Q1,R1);                 % Compute Control Gain Matr

%*************************************************************************
figure;
sv=sigma(ss(A_blin,H1,C_blin,D_blin),w);
tsv=20*log10(sv);
semilogx(w,tsv);
title('Target Loop (G_KF)');
grid on;
xlabel('Frequency (rad/sec)');
ylabel('Singular Values (dB)');

%*************************************************************************
tolpoles = eig(A_blin)                               % Target Open Loop Poles
targzeros = tzero(A_blin,H1,C_blin,0*ones(nc,nc))    % Target Open Loop Zeros
tclpoles = eig(A_blin H1*C_blin)                     % Target Closed Loop Poles

%*************************************************************************
figure
sv = sigma(ss(A_blin H1*C_blin, H1,  C_blin, eye(nc)),w);
sv = 20*log10(sv);
semilogx(w, sv)
%clear sv
title('Target Sensitivity (S_{KF}) Singular Values')
grid
xlabel('Frequency (rad/sec)')
ylabel('Singular Values (dB)')

sv = sigma(ss(A_blin H1*C_blin, H1, C_blin, 0*eye(nc)),w);
sv = 20*log10(sv);
figure
semilogx(w, sv, w, 20*log10(10./w))
title('Target Complementary (T_{KF}) Singular Values')
grid
xlabel('Frequency (rad/sec)')
ylabel('Singular Values (dB)')

%*************************************************************************
% Analysis LQG LTR
% Am1=A_blin  B_blin*G H1*C_blin;
% Bm1=H1;
```

```
% Cm1=G;
% Dm1=0;
% Gltr=ss(Am1,Bm1,Cm1,Dm1);
%Form final compensator
Am1 = [0*ones(2,2)   G1;
       0*ones(8,2)  A_blin  B_blin*G1 H1*C_blin];
Bm1 = [0*ones(2,2);
         H1];
Cm1 = [eye(2,2)  0*ones(2,8)]

Dm1 = [0*ones(2,2)];
Gltr=ss(Am1,Bm1,Cm1,Dm1);
ltrp=eig(Am1);
ltrtz=tzero(Gltr);

[ak,bk,ck,dk]=bilin(Gltr.A,Gltr.B,Gltr.C,Gltr.D, 1,'Sft_jw',[p2  p1]);
K3=ss(ak,bk,ck,dk);
[Lo3,Li3,So3,Si3,To3,Ti3,KS3,SP3]=f_CLTFM(P,K3);
%************************************************************************
%
% OPEN LOOP FREQUENCY RESPONSE
figure;
sigma(Lo3,w);
title('LQG LTR Loop Singular Values: Error Signal')
grid
xlabel('Frequency (rad/sec)')
ylabel('Singular Values (dB)')

figure;
sigma(Li3,w);
title('LQG LTR Loop Singular Values: Plant Input')
grid
xlabel('Frequency (rad/sec)')
ylabel('Singular Values (dB)')

%************************************************************************
%
% CLOSED LOOP FREQUENCY RESPONSE

figure;
sigma(So3,w);
title('LQG LTR: Sensitivity Error Signal')
grid
xlabel('Frequency (rad/sec)')
ylabel('Singular Values (dB)')

figure;
sigma(Si3,w);
title('LQG LTR: Sensitivity Plant Input')
grid
xlabel('Frequency (rad/sec)')
ylabel('Singular Values (dB)')

figure;
```

```
sigma(To3,w);
title('LQG LTR: Complementary Sensitivity Plant Output')
grid
xlabel('Frequency (rad/sec)')
ylabel('Singular Values (dB)')

figure;
sigma(Ti3,w);
title('LQG LTR: Complementary Sensitivity Plant Input')
grid
xlabel('Frequency (rad/sec)')
ylabel('Singular Values (dB)')

figure;
sv=sigma(KS3,w);
tsv=20*log10(sv);
semilogx(w,tsv);
title('K Sensitivity (KS) using LQG LTR');
grid on;
xlabel('Frequency (rad/sec)');
ylabel('Singular Values (dB)');
%*************************************************************************
% Time response
t = [0:0.02:10];
[y, t, x] = step(To3,t);
figure;
subplot(1,2,1)
plot(t,y(:,:,1))
grid
title('Velocity & FPA To r = [1  0]  Command')
ylabel('velocity & FPA (deg)')
xlabel('Time (seconds)')

t = [0:0.02:20];
[y, t, x] = step(To3,t);
subplot(1,2,2)
plot(t,y(:,:,2))
grid
title('Velocity & FPA To r = [0  1]  Command')
ylabel('velocity & FPA (deg)')
xlabel('Time (seconds)')
%*************************************************************************
%% H infinity Robust Constrol Design
% Weights
% Standard first order weights are chosen
% For any non standard/higher order weights, form the transfer functions
% appropiately
%*************************************************************************
% Visualizing the Weighting matrix for Robust control
%
M11=7; w11=0.01; Eps11=0.003; M12=7; w12=0.01; Eps12=0.003;
W1 = [tf([1/M11 w11], [1 w11*Eps11]) 0; 0 tf([1/M12 w12], [1 w12*Eps12])];
figure;
sigma(inv(W1),w)
```

```
title('Inverse of Weighting matrix W1');
grid on;
xlabel('Frequency (rad/sec)');
ylabel('Singular Values (dB)');
M21=0.1; w21=10; Eps21=0.01; M22=0.1; w22=10; Eps22=0.01;
W2 = [tf([1 w21/M21], [Eps21 w21]) 0; 0 tf([1 w22/M22], [Eps22 w22])] ;
figure;
sigma(inv(W2),w)
title('Inverse of Weighting matrix W2');
grid on;
xlabel('Frequency (rad/sec)');
ylabel('Singular Values (dB)');
M31=2; w31=20; Eps31=0.001; M32=2; w32=20; Eps32=0.001;
W3 = [tf([1 w31/M31], [Eps31 w31]) 0; 0 tf([1 w32/M32], [Eps32 w32])] ;
figure;
sigma(inv(W3),w)
title('Inverse of Weighting matrix W3');
grid on;
xlabel('Frequency (rad/sec)');
ylabel('Singular Values (dB)');
%************************************************************************
% M11=1.2; w11=0.01; Eps11=0.001; M12=1.2; w12=0.05; Eps12=0.001;
% W1 = [tf([1/M11 w11], [1 w11*Eps11]) 0 ; 0 tf([1/M12 w12] , [1 w12*Eps12])];
% figure;
% sigma(inv(W1),w)
% title('Inverse of Weighting matrix W1');
% grid on;
% xlabel('Frequency (rad/sec)');
% ylabel('Singular Values (dB)');
% M21=100; w21=1000; Eps21=0.01; M22=100; w22=1000; Eps22=0.01;
% W2 = [tf([1 w21/M21], [Eps21 w21]) 0 ; 0 tf([1 w22/M22], [Eps22 w22])] ;
% figure;
% sigma(inv(W2),w)
% title('Inverse of Weighting matrix W2');
% grid on;
% xlabel('Frequency (rad/sec)');
% ylabel('Singular Values (dB)');
% M31=1.6; w31=3; Eps31=0.001; M32=1.6; w32=18; Eps32=0.001;
% W3 = [tf([1 w31/M31], [Eps31 w31]) 0; 0 tf([1 w32/M32], [Eps32 w32])] ;
% figure;
% sigma(inv(W3),w)
% title('Inverse of Weighting matrix W3');
% grid on;
% xlabel('Frequency (rad/sec)');
% ylabel('Singular Values (dB)');

%************************************************************************
p11= 0.0944; p22= 1e20;
[A_blin1,B_blin1,C_blin1,D_blin1]=bilin(Ad,Bd,Cd,Dd,1,'Sft_jw',[p22 p11]);
Pd_lin1 = ss(A_blin1,B_blin1,C_blin1,D_blin1)
%************************************************************************
% % Generalized plant
% % Standard weight augmentation using Matlab's augw command
% % For any non standard augmentation of weights, form the Generalized plant
```

```
%% manually using state space methods
GenP=augw(Pd_lin1,W1,W2,W3);
Kd=hinfsyn(GenP);

[akd,bkd,ckd,dkd] = ssdata(Kd);
[ak4,bk4,ck4,dk4]=bilin(akd,bkd,ckd,dkd, 1,'Sft_jw',[p22 p11]);
Kh=ss(ak4,bk4,ck4,dk4);

[Lo4,Li4,So4,Si4,To4,Ti4,KS4,PS4] = f_CLTFM(Pd,Kh);
%%%%%%%%%%%%%%%%%%%%%%%%%%%%%%%%%%%%%%%%%%%%%%%%%%%%%%%%%%%%%%%%%%%%%%%%%%%
%Analysing system after H infinity design
%
% OPEN LOOP FREQUENCY RESPONSE
figure;
sigma(Lo4,w);
title('H infinity  Open_Loop_Singular_Values:_Error_Signal')
grid
xlabel('Frequency_(rad/sec)')
ylabel('Singular_Values_(dB)')

figure;
sigma(Li4,w);
title('H infinity  Open_Loop_Singular_Values:_Plant_Input')
grid
xlabel('Frequency_(rad/sec)')
ylabel('Singular_Values_(dB)')

%%%%%%%%%%%%%%%%%%%%%%%%%%%%%%%%%%%%%%%%%%%%%%%%%%%%%%%%%%%%%%%%%%%%%%%%%%%
%
% CLOSED LOOP FREQUENCY RESPONSE

figure;
sigma(So4,w);
title('H infinity  Sensitivity:_Error_Signal')
grid
xlabel('Frequency_(rad/sec)')
ylabel('Singular_Values_(dB)')

figure;
sigma(Si4,w);
title('H infinity  Sensitivity:_Plant_Input')
grid
xlabel('Frequency_(rad/sec)')
ylabel('Singular_Values_(dB)')

figure;
sigma(To4,w);
title('H infinity  Complementary_Sensitivity:_Plant_Output')
grid
xlabel('Frequency_(rad/sec)')
ylabel('Singular_Values_(dB)')

figure;
sigma(Ti4,w);
```

```
title('H infinity  Complementary Sensitivity: Plant Input')
grid
xlabel('Frequency (rad/sec)')
ylabel('Singular Values (dB)')

figure;
sv=sigma(KS4,w);
tsv=20*log10(sv);
semilogx(w,tsv);
title('K Sensitivity (KS) using H infinity');
grid on;
xlabel('Frequency (rad/sec)');
ylabel('Singular Values (dB)');

%%
%%%%%%%%%%%%%%%%%%%%%%%%%%%%%%%%%%%%%%%%%%%%%%%%%%%%%%%%%%%%%%%%%%%%%%%%%%%%%%%
%
% CLOSED LOOP TIME RESPONSE
t = [0:0.02:150];
[y, t, x] = step(To4,t);

% PITCH COMMAND
% Pitch: r = [ 1   0 ] Pitch Command

figure;
subplot(1,2,1)
%step(To4)
plot(t,y(:,:,1))
grid
title('Pitch & Gamma Response To r = [1  0]  Command')
ylabel('Theta & Gamma (deg)')
xlabel('Time (seconds)')
subplot(1,2,2)
plot(t,y(:,:,2))
grid
title('Pitch & Gamma Response To r = [0  1]  Command')
ylabel('Theta & Gamma (deg)')
xlabel('Time (seconds)')
%
%end
```